United States
Environmental Protection
Agency

National Risk Management
Research Laboratory
Ada, OK 74820

Research and Development

EPA/600/S-99/001

February 1999

ENVIRONMENTAL RESEARCH BRIEF

Colloid Mobilization and Transport in Contaminant Plumes: Field Experiments, Laboratory Experiments, and Modeling

Joseph N. Ryan[1], Rebecca A. Ard[1], Robin D. Magelky[1],
Menachem Elimelech[2], Ning Sun[2], and Ne-Zheng Sun[2]

Abstract

The major hypothesis driving this research, that the transport of colloids in a contaminant plume is limited by the advance of the chemical agent causing colloid mobilization, was tested by (1) examining the dependence of colloid transport and mobilization on chemical perturbations, (2) assessing the relative transport of mobilized colloids and the chemicals that caused their mobilization, and (3) developing a colloid transport model that would begin to describe these effects. Through field tests, laboratory experiments, and model development, we made significant advances toward the testing of the hypothesis. The field tests, conducted in the uncontaminated and contaminated zones of a ferric oxyhydroxide-coated quartz sand aquifer, showed in almost all cases that colloids will not advance ahead of the plume that caused their mobilization. The laboratory experiments showed chemical perturbations that cause increasingly repulsive conditions produced more extensive and more rapid colloid release. In both the field and laboratory experiments, good correlations were observed between the surface properties of the colloid and aquifer grains and their transport and mobilization behavior. The colloid transport model was developed to describe colloid transport in physically and geochemically heterogeneous porous media similar to that encountered at the field site. The model results showed that physical and geochemical heterogeneities could result in preferential flow of colloids in layered porous media, while random distributions of the two heterogeneities, especially the physical heterogeneity, lead to a random behavior of colloid transport.

Introduction

Colloids have been implicated in the enhanced transport of radionuclides and metals in recent field studies and laboratory experiments [Buddemeier and Hunt, 1988; McCarthy and Zachara, 1989; Dunnivant et al., 1992; Puls and Powell, 1992; Grolimund et al., 1996]. Unfortunately, these studies have rarely delved into the genesis, nature, and abundance of the colloids responsible for the enhanced transport. We are relatively certain of the processes governing the association of these contaminants with colloids, but we have little knowledge of the potential for colloid mobilization and subsequent transport in a given aquifer.

Colloid mobilization is caused by chemical and physical perturbations to aquifer geochemistry and hydraulics [McCarthy and Degueldre, 1993; Ryan and Elimelech, 1996]. Chemical perturbations of the type occurring in contaminant plumes are capable of mobilizing large quantities of colloids. In particular, the mobilizing effect of organic compounds like surfactants and reductants is well known [Ryan and Gschwend, 1994; Allred and Brown, 1994]. Colloid mobilization by physical perturbations is generally limited to fracture flow and increases in groundwater flow velocity induced by pumping [Degueldre et al., 1989; Puls et al., 1992; Backhus et al., 1993].

[1] *Department of Civil, Environmental, and Architectural Engineering, University of Colorado, Boulder.*
[2] *Department of Civil and Environmental Engineering University of California, Los Angeles.*

In contaminant plumes, colloids are mobilized and transported with the groundwater. If the advance of the contaminant plume is retarded, the colloids will attempt to move ahead of the plume. When the colloids re-enter the pristine groundwater, they will be redeposited. As the plume catches up, the colloids will be remobilized and the cycle will begin again. These simultaneous mobilization and deposition processes have been observed in natural analogs to contaminant plumes like organic matter-rich water infiltrating from a swamp [Ryan and Gschwend, 1990] or fresh water advancing into salt water in a coastal aquifer [Goldenberg et al., 1983]. The major hypothesis of this research was that the transport of the colloids in a contaminant plume is limited by the advance of the chemical agent causing colloid mobilization. To design experiments to test this hypothesis, we set three overall objectives for the project: (1) examine the dependence of colloid transport and mobilization on chemical perturbations, (2) assess the relative transport of mobilized colloids and the chemicals that caused their mobilization, and (3) develop a colloid transport model that would begin to describe these effects. These objectives were met and the hypothesis was tested by field experiments at the U.S. Geological Survey Cape Cod aquifer site, laboratory mobilization experiments, and the development of a colloid transport model emphasizing the dynamics of colloid transport and the effects of heterogeneity.

Field Experiments

Purpose

Two field experiments were conducted during the summers of 1996 and 1997 at the U.S. Geological Survey's Toxic Substances Hydrology Research Site on Cape Cod, Massachusetts. To address two of the overall objectives of the project, to examine the dependence of colloid transport and mobilization on chemical perturbations and to assess the relative transport of mobilized colloids and the chemicals that caused their mobilization, the following tests were conducted in the field:

- assessment of the effects of chemical perturbations (elevated pH, surfactant concentration, and reductant concentration and decreased ionic strength) on the mobilization of natural colloids, synthetic colloids, and viruses
- measurement of the rate of deposition of synthetic colloids and viruses
- determination of the relative rates of migration of a plume of a colloid-mobilizing agent and the mobilized colloids

In addition, we demonstrated the use of silica-coated metal oxide tracer colloids in a field experiment unrelated to the original overall goals of the project.

These experiments were conducted in the field (rather than in the laboratory) for three major reasons. First, we expect that the extent of colloid mobilization from a sediment would increase with disturbances to the sediment like sampling, repacking into columns, and drying. Measurement of the extent of colloid mobilization *in situ* should provide a more realistic estimate of the effect of chemical perturbations on colloid mobilization. Second, the Cape Cod site provided a unique opportunity to observe colloid mobilization and transport in a relatively homogeneous aquifer with a clear geochemical difference imposed by a plume of secondarily-treated sewage; reproducing such a system in the laboratory would be very difficult. Third, we hypothesized that detection of the relative rate of migration of a colloid-mobilizing agent (e.g., elevated pH, surfactant) and the mobilized colloids would require monitoring of transport of a distance of a few meters. The Cape Cod site provided well-instrumented arrays of multi-level samplers for injection and monitoring to test this hypothesis.

Site Description

The virus and silica colloid injections were conducted in the surficial aquifer at the U.S. Geological Survey's Cape Cod Toxic Waste Research Site near the Massachusetts Military Reservation on Cape Cod, Massachusetts. The aquifer was contaminated by disposal of secondary sewage effluent onto rapid infiltration sand beds for over 50 years [LeBlanc, 1984], creating a contaminant plume characterized by low dissolved oxygen concentrations and elevated pH, specific conductivity, and organic carbon concentrations (Table 1). Previously, the site has been used to study the transport of groundwater tracers, metals, nutrients, detergents, microspheres, bacteria, protozoa, and viruses [Barber et al., 1988; Harvey et al., 1989; 1995; Harvey and Garabedian, 1991; Smith et al., 1991; Hess et al., 1992; Kent et al., 1994; Bales et al., 1995; Pieper et al., 1997]. The aquifer consists of Pleistocene glacial outwash deposits characterized by interbedded lenses of sand and gravel. The grains (average diameter 0.6 mm) consist mainly of quartz coated by ferric oxyhydroxides [Coston et al., 1995]. The effective porosity is 0.39 and the average hydraulic conductivity is 110 m d^{-1}. The water table depth is between 6 m and 7 m below the surface near the study site [LeBlanc et al., 1991].

Groundwater at the site is monitored by approximately 1,000 multi-level samplers (MLSs), each consisting of a bundle of polyethylene tubes threaded through a polyvinylchloride pipe to 15 depths below the water table at 25 cm depth intervals. In the direction of groundwater flow, these MLSs are spaced at 1m to 2 m distances. For our studies, we used three small arrays of MLSs near the up-gradient end of the site (Figure 1).

Materials and Methods

The following section highlights important aspects of the materials used and methods followed during the field experiments. Details are provided in Ard [1997] and Magelky [1998].

Injections. Two major sets of field experiments were conducted during the summers of 1996 [Ard, 1997] and 1997 [Magelky, 1998]. Each set of experiments consisted of (1) natural colloid mobilization by chemical perturbations, (2) synthetic colloid deposition under ambient conditions, and (3) synthetic colloid mobilization by chemical perturbations. Injections of 100 L of amended groundwater were made into the uncontaminated and contaminated zones of the aquifer using four arrays of multi-level samplers (MLSs). Each MLS array consisted of an injection MLS and four to six monitoring MLSs at down-gradient intervals of approximately 1 m. In 1996, three identical virus and colloid injections were followed by three different chemical perturbation injections (Table 2). In 1997, a variety of colloid and chemical perturbation injections were made (Table 3).

Sampling and Field Analysis. During both field experiments, six depths in each of the MLSs were sampled immediately before and after the injections to measure background and initial concentrations (C_0) for each constituent. After the injections, samples were collected daily (1996) or twice daily (1997). In the field, sample pH, specific conductance, dissolved oxygen, and ferrous iron were measured. The pH meter and electrode were calibrated with pH 4, 7, and 10 buffers at the groundwater temperature and calibrations varying by more than 5% from the proper Nernst response were redone. The specific conductance electrode and meter were calibrated with solutions of known conductance at the groundwater temperature. Calibrations varying by more than 5% from the known conductances were redone. The dissolved oxygen measurements, made by Rhodazine D™ (0 to 1 mg L^{-1}) and indigo carmine (1 to 12 mg L^{-1}) test kits (CHEMetrics, Inc.), were checked against solutions purged by

Table 1. Chemistry of the groundwater in the unconfined glacial outwash aquifer approximately 150 m downstream of the sewage infiltration beds at the Cape Cod site.

constituent	unit	uncontaminated zone	contaminated zone	reference
pH		5.4 to 5.6	5.8 to 6.0	this study
specific conductance	$\mu S\ cm^{-1}$	30 to 40	250 to 330	this study
ionic strength	mM	0.5	4.0	this study
temperature	^oC	15.5	15.0	this study
dissolved oxygen	$mg\ L^{-1}$	4.5 to 6.5	0 to 0.5	this study
dissolved organic carbon	$mg\ L^{-1}$	0.4 to 1.0	2.0 to 4.4	this study
MBAS[a]	$mg\ L^{-1}$	0.05	0.10	this study
Na^+	μM	250	1,900	this study
K^+	μM	21	200	LeBlanc et al. [1991]
Mg^{2+}	μM	37	130	LeBlanc et al. [1991]
Ca^{2+}	μM	28	210	this study
NH_4^+	μM	<1	<1	LeBlanc et al. [1991]
Mn (dissolved)	μM	0.64	15	LeBlanc et al. [1991]
Fe (dissolved)	μM	<0.05	0.16	this study
Cl^-	μM	230	760	LeBlanc et al. [1991]
NO_3^-	μM	<10	300	LeBlanc et al. [1991]
HCO_3^-	μM	28	640	LeBlanc et al. [1991]
SO_4^{2-}	μM	85	360	LeBlanc et al. [1991]
total PO_4^{3-}	μM	0.74	12	LeBlanc et al. [1991]
sediment clay content	wt %	0.33±0.02	0.35±0.06	this study
sediment Fe(III)[b]	$\mu mol\ g^{-1}$	3.6±0.3	4.7±1.4	this study
sediment phosphate	$\mu mol\ g^{-1}$	0.61±0.09	0.58 to 1.5	Walter et al. [1996]
sediment f_{oc}		<0.0001	0.01	Scholl and Harvey [1992]

[a] *MBAS, methylene blue active substances (detergents, surfactants).*
[b] *Sediment Fe(III) is ferric iron extracted by Ti(III)-citrate-EDTA-bicarbonate [Ryan and Gschwend, 1991].*

nitrogen and saturated by air at the groundwater temperature. Ferrous iron measurements, made by a 1,10-phenanthroline 0.1 to 10 mg L^{-1} test kit (CHEMetrics, Inc.), were checked against 0.1 and 1.0 mg L^{-1} $FeCl_2$ solutions prepared in the field laboratory.

Injection Constituents. Bromide, added as NaBr, was used as a conservative tracer and measured by ion-specific electrode. The bromide electrode was calibrated by 0.01, 0.1 and 1.0 mM sodium bromide solutions before and after each set of measurements. Calibration curves showing 5% variation from the proper Nernst response were redone. Sodium hydroxide was added after dissolution in 1 L of deionized water (Millipore Milli-Q) to elevate pH. Sodium dodecylbenzenesulfonate (NaDBS) dissolved in high purity water was added to elevate the surfactant concentration and measured with a methylene blue active substances (MBAS) test kit (Hach Co.) with a detection limit of 0.1 mg L^{-1}. The MBAS test kit was tested against NaDBS solutions of known concentration. *L*-ascorbic acid dissolved in deionized water was added to elevate the reductant concentration. Ascorbic acid concentrations were measured by UV spectrophotometry at 264 nm checked against standards made in uncontaminated and contaminated groundwater. To reduce the ionic strength of the groundwater, injections of deionized water were made and tracked by specific conductance.

Silica colloids (Nissan Chemical Industries, MP-1040) of 107±21 nm diameter were used as the synthetic colloid during the 1996 experiments. Silica colloid concentration was measured by UV spectrophotometry at 340 nm (with a detection limit of about $C\ C_0^{-1}$=0.001) and turbidity (with a detection limit of about $C\ C_0^{-1}$=0.01). The spectrophotometer and turbidity meter were calibrated using silica colloid suspensions in the uncontaminated and contaminated groundwaters. The silica colloids were chosen to mimic the negative surface charge found on most natural colloids and to provide a uniform colloid size distribution for which to assess the collision efficiency.

To improve the detection of the colloids injected during our 1997 field experiment, two “tracer” colloids composed of metal oxides (zirconia, ZrO_2; titania, TiO_2) coated by silica were developed [Ryan, Magelky, and Elimelech, in preparation]. The

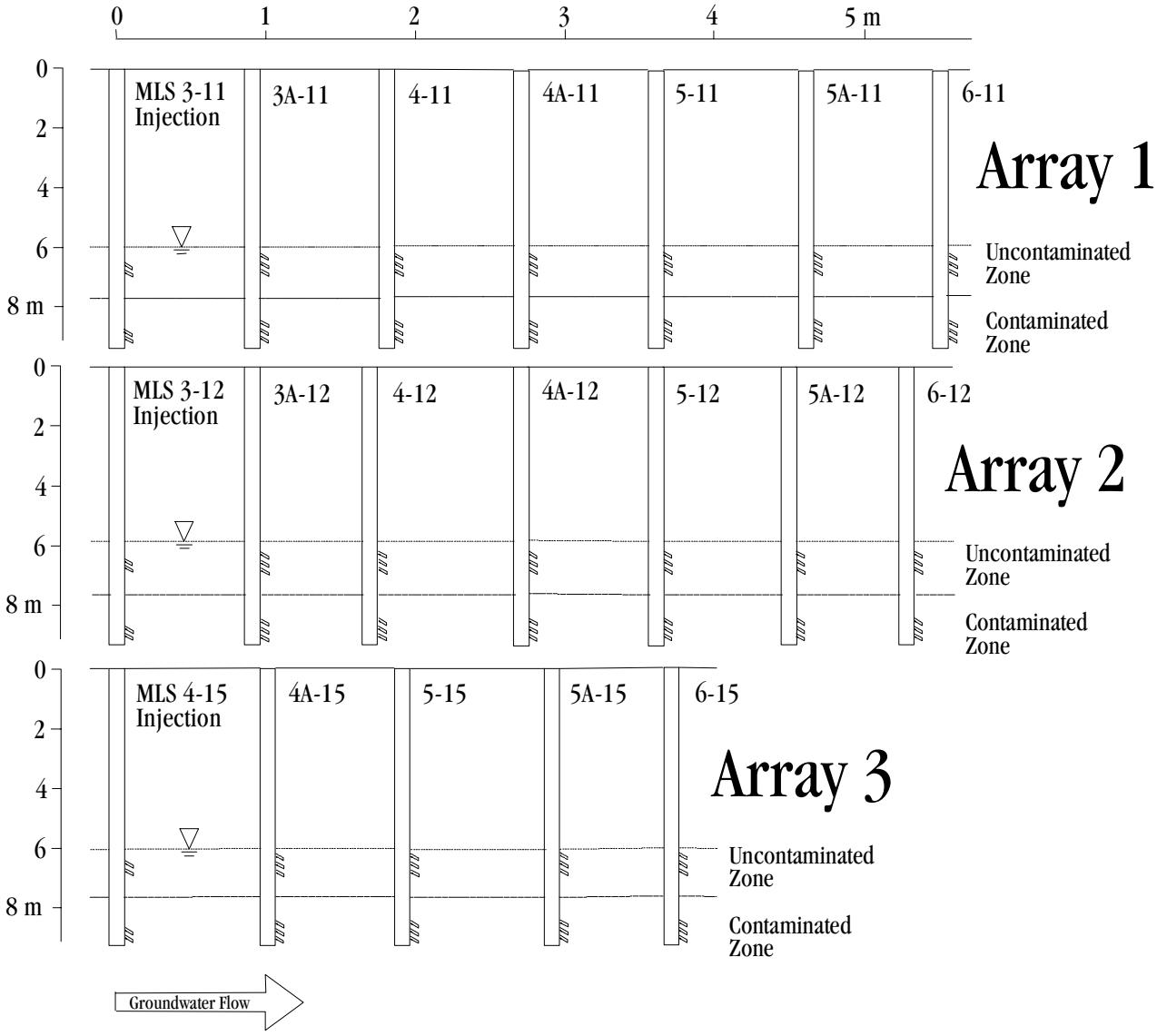

Figure 1. Sketch of multilevel sampler (MLS) arrays used in the field experiments at the Cape Cod site. Array numbering shown for 1996 experiments. For 1997 experiments, Array 1 is headed by MLS 3-11, Array 2 is headed by MLS 4-11, Array 3 is headed by MLS 3-12, and Array 4 is headed by MLS 4-15. Sampling ports are separated by 25 cm depths. Depths to the water table and the boundary between the uncontaminated and contaminated groundwater are shown.

zirconia particles were purchased from Aldrich Chemical Co. in an acetic acid solution. The titania particles were synthesized by the hydrolysis of titanium(IV)tetraethoxylate in a mixture of water in ethanol (1% v/v) and hydroxypropyl cellulose. The zirconia and titania particles were coated with silica by hydrolysis of tetramethyl orthosilicate (Table 4). The concentrations of the silica-coated zirconia and titania particles were measured by inductively-coupled plasma-atomic emission spectrophotometry for zirconium and titanium, providing a much improved detection limit of $C\,C_0^{-1} < 10^{-5}$ owing to the very low background concentrations of zirconium and titanium. A particle nebulization efficiency factor was established by comparing instrument response to the pure zirconia and titania particles to acidified solutions of Zr and Ti ions. The silica coatings on these particles mimic the negative charge found on most natural particles (as did the pure silica particles) and the relatively uniform size distributions foster accurate collision efficiency calculations and modeling.

The virus used in the injections is the bacteriophage PRD1 [Olsen et al., 1974]. The PRD1 were radiolabeled with ^{32}P-phosphate [Loveland et al., 1996]. PRD1, which was isolated from municipal sewage, has a negative surface charge and size typical of many pathogenic waterborne viruses. Virus concentrations were measured by liquid scintillation counting and checked by standards of known ^{32}P activity.

Colloid Characterization. The abundance of natural colloids was measured by turbidity. Turbidity was converted to a colloid concentration by measuring the mass of colloids in samples of known turbidity. The natural colloids were also characterized by

Table 2. Summer 1996 injection schedule. Constituents of natural colloid mobilization and silica colloid and bacteriophage PRD1 deposition and recovery experiments. C_0 is the concentration measured in samples withdrawn immediately after injection.

injection	array	constituents	injectate concentration	uncontaminated C_0 6.4 m depth	contaminated C_0 8.7 m depth
natural colloid mobilization	1	NaOH	pH 12.5	pH 12.3	pH 11.9
		NaBr	1.50 mM	1.18 mM	1.46 mM
	2	NaDBS[a]	0.57 mM	0.34 mM	0.66 mM
		NaCl	2.56 mM	2.13 mM	2.47 mM
	3	ascorbic acid	1.82 mM	0.63 mM	1.73 mM
		NaBr	1.50 mM	1.33 mM	1.56 mM
synthetic colloid deposition	1	PRD1	2.6×10^6 cpm L^{-1}	1.3×10^6 cpm L^{-1}	1.9×10^6 cpm L^{-1}
		SiO_2 colloids	500 mg L^{-1}	390 mg L^{-1}	470 mg L^{-1}
		NaBr	1.50 mM	0.79 mM	0.90 mM
	2	PRD1	2.1×10^6 cpm L^{-1}	1.5×10^6 cpm L^{-1}	1.8×10^6 cpm L^{-1}
		SiO_2 colloids	500 mg L^{-1}	400 mg L^{-1}	480 mg L^{-1}
		NaBr	1.50 mM	1.05 mM	1.12 mM
	3	PRD1	2.2×10^6 cpm L^{-1}	1.3×10^6 cpm L^{-1}	1.7×10^6 cpm L^{-1}
		SiO_2 colloids	500 mg L^{-1}	210 mg L^{-1}	310 mg L^{-1}
		NaBr	1.50 mM	0.90 mM	1.02 mM
synthetic colloid recovery	1	NaOH	pH 12.5	pH 11.7	pH 11.8
		NaBr	1.50 mM	0.77 mM	1.04 mM
	2	NaDBS	57 mM	52 mM	52 mM
		NaBr	1.50 mM	1.36 mM	1.07 mM
	3	ascorbic acid	1.82 mM	1.76 mM	2.09 mM
		NaBr	1.50 mM	0.86 mM	1.11 mM

[a] *NaDBS is sodium dodecylbenzene sulfonate, an anionic surfactant.*

Table 3. Summer 1997 injection schedule. Constituents of natural colloid mobilization and silica-coated zirconia and titania colloid deposition and recovery experiments. C_0 is the concentration measured in samples withdrawn immediately after injection. Silica-coated zirconia and titania colloids are shown as Si/ZrO_2 and Si/TiO_2, respectively.

injection	array	constituents	injectate concentration[a]	uncontaminated C_0 6.4 m depth	contaminated C_0 8.7 m depth
natural colloid mobilization	1	NaOH	pH 11	pH 10.3	pH 10.8
		NaBr	1.00 mM	0.75 mM	0.72 mM
	3	deionized water[b]			
	4	NaDBS[c]	29 mM	43 mM	11 mM
		NaBr	1.00 mM	0.34 mM	0.75 mM
synthetic colloid deposition	1	Si/ZrO_2	249/230 ppm Zr	190 ppm	51.9 ppm
		NaBr	1.00 mM	1.11 mM	1.11 mM
	2	Si/ZrO_2	261/275 ppm Zr	191 ppm	159 ppm
		NaBr	1.00 mM	0.99 mM	0.69 mM
	3	Si/ZrO_2	246/234 ppm Zr	283 ppm	240 ppm
		NaBr	1.00 mM	0.92 mM	0.94 mM
	4	Si/ZrO_2	61/124 ppm Zr	62.7 ppm	33.0 ppm
		Si/TiO_2	93/140 ppm Ti	41.0 ppm	41.1 ppm
		NaDBS	72 µM	72 µM	72 µM
		NaBr	1.00 mM	1.04 mM	1.11 mM
1st synthetic colloid recovery	1	NaOH	pH 11	pH 10.8	pH 11.2
		NaBr	1.00 mM	0.87 mM	0.81 mM
	3	deionized water			
2nd synthetic colloid recovery	3	NaOH	pH 10	pH 9.7	pH 9.7
		NaBr	1.00 mM	1.09 mM	1.01 mM

[a] *Injectate concentration in uncontaminated and contaminated zones shown as "uncont/cont" where the concentrations were different in the two injectates.*
[b] *Millipore Milli-Q®-prepared water used as deionized water.*
[c] *NaDBS is sodium dodecylbenzene sulfonate, an anionic surfactant.*

Table 4. Size of titania and zirconia particles before and after coating with silica. Size measured by dynamic light scattering reported as the mean diameter ± one standard deviation for a Gaussian distribution of particle sizes.

particle	uncoated diameter (nm)	silica-coated diameter (nm)	silica coating thickness[a] (nm)
zirconia	110 ±34	130 ±49	10
titania	1030±140	1080±160	50

[a] *Coating thickness estimated as one-half the difference between the silica-coated and uncoated diameters.*

SEM and energy-dispersive x-ray spectroscopy (EDX) after being trapped on filters, mounted on aluminum stubs, and gold- or carbon-coated. The electrophoretic mobility of the colloids and virus were determined by microelectrophoresis (Brookhaven, model ZetaPlus) in uncontaminated and contaminated groundwater and groundwaters amended by the chemical perturbations. The consistency of microelectrophoresis measurements was checked by measuring the zeta potential of polystyrene latex microspheres. During the elevated pH mobilization experiments in 1997, dissolved organic carbon was measured in 0.45µm-filtered samples by combustion on a platinum catalyst (Shimadzu TOC-5000). The organic carbon analyzer response was calibrated with potassium biphthalate solutions. Total organic carbon concentration was also measured by absorbance of light at 254 nm in unfiltered samples.

Aquifer Sediments. Cores were obtained from the uncontaminated and contaminated zones of the aquifer about 5 m east of the injection wells used in the field experiments. The sediments were impregnated with epoxy resin and thin-sectioned for electron microprobe (JEOL, model 8600, 15 kV accelerating voltage) and SEM (backscatter electron detection) analysis. The area of surfaces covered by ferric oxyhydroxide coatings were estimated by observing the fraction of surface coatings for 400 grains in the uncontaminated and contaminated zone sediments. The mineralogy of the fine particles of the sediments was determined by powder x-ray diffraction (XRD). Total Fe, Al, and Mn were measured by digestion in concentrated HF/HNO_3 solutions. Free Fe, Al, Mn were measured by Ti(III)-citrate-EDTA-bicarbonate extraction [Ryan and Gschwend, 1991]. The total digestions and free element extractions were checked by measuring the Fe, Al, and Mn content of pure oxides of these elements. The streaming potentials of aquifer grains were measured in the laboratory of Dr. Philip R. Johnson at Notre Dame University.

Data Quality Assurance. The data collected in the field were subject to careful quality assurance procedures outlined in the *Quality Assurance Project Plan for Colloid Mobilization and Transport in Contaminant Plumes*, a report prepared by the project investigators at the beginning of the project. All of the data presented in this report met the data quality assurance criteria.

Specific quality assurance procedures have been included with the details of analysis above. In addition to these specific procedures, many general quality assurance procedures were followed. Analytical methods used to characterize the sediment and groundwater samples were tested using standards and spiked samples. Selected samples were measured on alternate instruments available in nearby laboratories (particle size, zeta potential) for analyses that cannot be absolutely calibrated or tested for accuracy. The influence of contamination from reagents and laboratory environment was assessed using reagent blanks and method blanks. Instrument variability was tested with internal standards. Measurements were checked by mass balance. During fieldwork, field blanks were included in the samples to assess contamination of samples by sample containers, sampling handling, storage, and shipping. Preliminary studies were carried out to determine the primary sources of error in analytical procedures. In both the laboratory and the field, replicate samples were tested at various times to assess the effect of sample aging and storage on results.

Calculation of Attenuation, Collision Efficiency, Recovery, and Interaction Forces. The relative breakthrough (RB, %) of an injected constituent is a ratio of the time-integrated mass of the constituent relative to that of the conservative tracer. Collision efficiencies (α) were calculated with longitudinal dispersion for pulse inputs of PRD1 and silica colloids [Harvey and Garabedian, 1991]. In the collision efficiency calculations, the single collector efficiencies [Yao et al., 1971; Rajagopalan and Tien, 1976] were calculated using only the convective-diffusion and sedimentation contributions. An average grain diameter of 0.6 mm, a porosity of 0.39, and fluid velocities of 0.7 m d^{-1} for the uncontaminated zone and 0.4 m d^{-1} for the contaminated zone were used in these calculations. Fractional recoveries of virus and silica colloids following the chemical perturbations were estimated as the quantity of virus or colloid recovered during the second injection divided by the quantity of virus or colloid immobilized during the first injection [Pieper et al., 1997].

Results

Colloid Characterization. The mobilized natural colloids ranged in size from <0.1 to 10µm, were platy in shape, and were composed primarily of silica and aluminum with traces of phosphorus and iron. No significant differences were observed for colloids mobilized in the uncontaminated or contaminated zones or for colloids mobilized by different chemical perturbations. Mineral identification by XRD revealed quartz, feldspar, kaolinite, illite/muscovite, and smectite, but no crystalline ferric oxyhydroxides. Microelectrophoresis analysis revealed a pH_{pzc} of approximately 2.2±0.3. Above pH 9.5, the zeta potentials of the colloids reached a plateau of about -45 mV.

The silica and silica-coated colloid surfaces were negatively charged from about pH 3 to the ambient pH of the uncontaminated groundwater (Tables 5 and 6). The silica and silica-coated colloids were slightly more negatively charged in the contaminated groundwater than in the uncontaminated groundwater.

The PRD1 surface was negatively charged from pH 3.2 to the ambient pH of the uncontaminated groundwater (Table 7). PRD1 was slightly more negatively charged in the contaminated groundwater than in the uncontaminated groundwater. The PRD1

Table 5. Silica-coated zirconia colloid zeta potentials under ambient and perturbed conditions.

sample	conditions		zeta potential (mV)
silica-coated ZrO_2 colloids	pH	3.0	-16±4
uncontam groundwater		4.0	-18±3
1.5 mM NaBr		5.0	-19±4
		6.0	-21±2
		7.0	-20±2
		8.0	-25±7
		9.0	-21±2
		10.0	-23±2
		11.0	-35±5
silica-coated ZrO_2 colloids	ambient		-21±2
uncontam groundwater	1 mM NaBr		-23±1
	72 µM NaDBS		-22±2
	49 mM NaDBS		-40±2
	1 mM AscAc		-24±3
	pH 10.0		-23±2
	pH 11.0		-35±4
silica-coated ZrO_2 colloids	pH	3.0	-20±4
contam groundwater		4.0	-20±2
1.5 mM NaBr		5.0	-21±2
		6.0	-19±1
		7.0	-22±2
		8.0	-23±2
		9.0	-21±3
		10.0	-24±2
		11.0	-26±2
silica-coated ZrO_2 colloids	ambient		-20±1
contam groundwater	1 mM NaBr		-24±2
	72 µM NaDBS		-22±1
	49 mM NaDBS		-40±2
	1 mM AscAc		-25±4
	pH 10.0		-24±1
	pH 11.0		-26±2

Table 6. Silica-coated titania zeta potentials under ambient and perturbed conditions.

sample	conditions		zeta potential (mV)
titania (TiO_2) colloids	pH	3.2	9±2
1.5 mM NaBr		4.0	4±3
		4.5	-8±1
		6.1	-23±2
		9.6	-28±5
		10.0	-26±2
silica-coated TiO_2 colloids	pH	3.1	1±2
1.5 mM NaBr		3.8	-7±3
		4.1	-13±2
		5.9	-27±2
		7.6	-22±4
		9.5	-27±4
		11.2	-25±2

Table 7. Bacteriophage PRD1 zeta potentials under ambient and perturbed conditions.

sample	conditions		zeta potential (mV)
PRD1	pH	3.2	-8±3
uncontam groundwater		4.1	-11±3
1.5 mM NaBr		5.2	-17±2
		6.1	-25±4
PRD1	pH	6.4	-27±4
contam groundwater			
1.5 mM NaBr			

zeta potentials are slightly more negative than those measured for PRD1 in a calcium phosphate solution [Bales et al., 1991].

Sediment Characterization. XRD revealed that the sediments were composed mostly of quartz, feldspars, and traces of clay minerals (kaolinite, illite/muscovite, smectite) and iron oxyhydroxides. Electron microprobe analysis of sediment thin sections from both the uncontaminated and contaminated zones revealed scattered coatings on the quartz grains that contained iron oxyhydroxide and clay minerals in both the uncontaminated and contaminated zones (Figure 2). The coating coverage was estimated at 3.0±10.0% of the uncontaminated grain surfaces and 3.5±11.1% of the contaminated grain surfaces. Most of the grains were uncoated and a small fraction of the grains were coated an average of about 50%. This small amount of surface coverage agrees well with the relatively low sediment Fe(III) concentrations measured by reductive extraction in the aquifer sediments (Table 1). The zeta potential of contaminated sediments in the contaminated groundwater is significantly more negative than that of the uncontaminated sediments in the uncontaminated groundwater (Table 8). The natural colloids mobilized from the uncontaminated sediments were characterized by a pH_{pzc} of about 2.3 and the chemical perturbations increased their negative charge (Table 9).

Natural Colloid Mobilization by Chemical Perturbations. Over the two field seasons, two injections of elevated pH groundwater were performed at approximate injection pH values of 11 (1997) and 12.5 (1996). The amount of colloids mobilized increased with increasing pH (Table 10). Colloid mobilization in the uncontaminated zone always exceeded colloid mobilization in the contaminated zone. The pH increase was buffered to a much greater extent in the contaminated zone. The appearance of the elevated pH plume and the mobilized colloids lagged the tracer breakthrough in these experiments. Details of the effect of pH on natural colloid mobilization will be presented in Ryan, Ard, Magekly, and Elimelech [in preparation].

During the 1996 experiment, the lower concentration of NaDBS (0.57 mM, 200 mg L^{-1}), about half the critical micelle concentration, caused greater mobilization of natural colloids in the uncontaminated zone. Owing to the presence of bubbles at the high NaDBS concentration (50 mM, 1%), we were not able to accurately measure turbidity during the 1997 experiment. At the lower concentration, a measurable amount of the NaDBS was attenuated, presumably by sorption to the aquifer sediments, but the overall transport of the NaDBS plume was not significantly retarded; thus, colloid mobilization coincided or slightly lagged the passage of the tracer and NaDBS pulses.

During the 1996 experiment, an increase in the ascorbic acid concentration produced much greater colloid mobilization in the uncontaminated zone than in the contaminated zone. Ascorbic acid was attenuated to $C\,C_0^{-1}$ levels of 0.05 and 0.5 in the uncontaminated and contaminated zones of the aquifer, respectively, but no significant retardation was observed. The mobilized colloids appeared at the same time or slightly behind the tracer and ascorbic acid pulses. Iron(II) concentrations well above the field detection limit of 1.8 μM were detected only in the contaminated zone.

During the 1997 experiment, a decrease in the ionic strength of the groundwater produced a small amount of colloid mobilization with slightly greater mobilization occurring in the uncontaminated zone. The deionized water "plume" moved through the array at the same rate as the bromide tracer moved through the array in later experiments and the mobilized colloids always appeared at the same time or slightly after the depression of specific conductance caused by the deionized water pulse.

Synthetic Colloid and Virus Deposition. During the 1996 experiments, silica colloids and bacteriophage PRD1 displayed measurable breakthroughs over the first meter of transport (Figure 3). Clear breakthrough curves were not detected further down-gradient [Ard, 1997]. The silica colloids and PRD1 were less attenuated in the contaminated zone than in the uncontaminated zone (Table 11). Collision efficiencies calculated with and without dispersion varied by up to a factor of 3.4 with the collision efficiency calculated with dispersion always the larger value. Details of these experiments are presented in Ryan, et al., [1998].

During the 1997 experiments, the transport of the silica-coated zirconia displayed similar trends in the same arrays – relative breakthroughs were higher and collision efficiencies were lower in the contaminated zone of the aquifer. Again, clear breakthroughs were not evident beyond the 1 m transport distance [Magelky, 1998]. In a special experiment conducted in 1997, both the silica-coated zirconia and titania particles were injected into array 4 following the injection of 29 mM (1%) NaDBS to mobilize natural colloids. Under these conditions, transport through the uncontaminated and contaminated zones was similar. The silica-coated zirconia colloids displayed collision efficiencies that were substantially lower than those of the silica-coated titania colloids.

Synthetic Colloid and Virus Mobilization. The amount of colloids and viruses mobilized by pH elevation increased as the pH of the injection was increased from 10 to 12.5 (Table 12). Generally, the pH increase was more effective at mobilizing colloids in the uncontaminated zone (Figure 4). The migration of the NaOH plume lagged significantly behind the tracer, but during the pH 11 injection in 1997, some of the mobilized colloids appeared slightly ahead of the pH increase at the 1 m transport distance (Figure 5). Dissolved organic carbon mobilized by this pH increase also appeared slightly ahead of the pH increase. Details of this work will be provided in Ryan, et al. [in preparation].

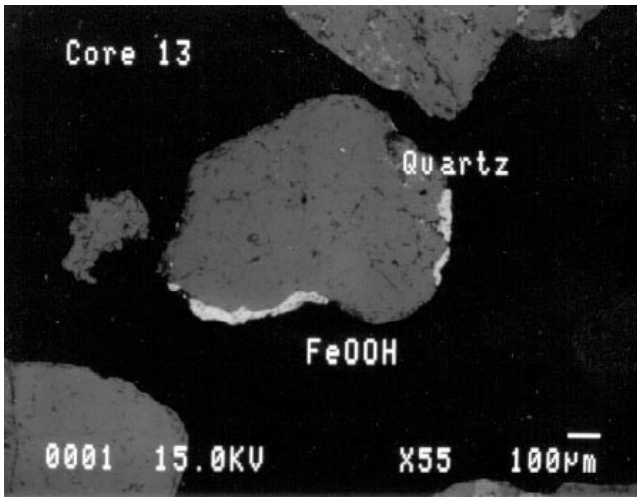

(a)

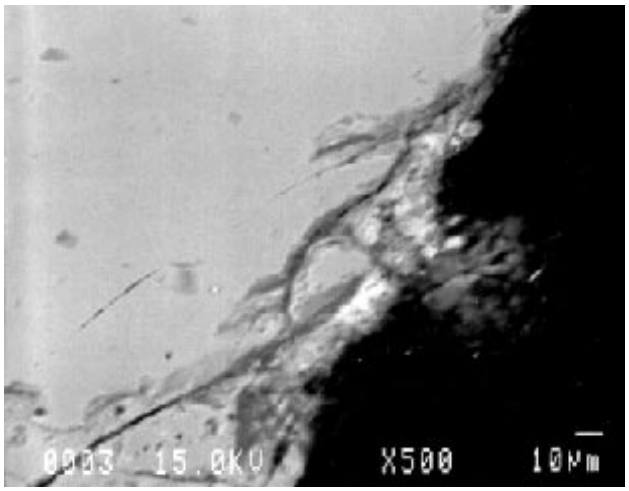

(b)

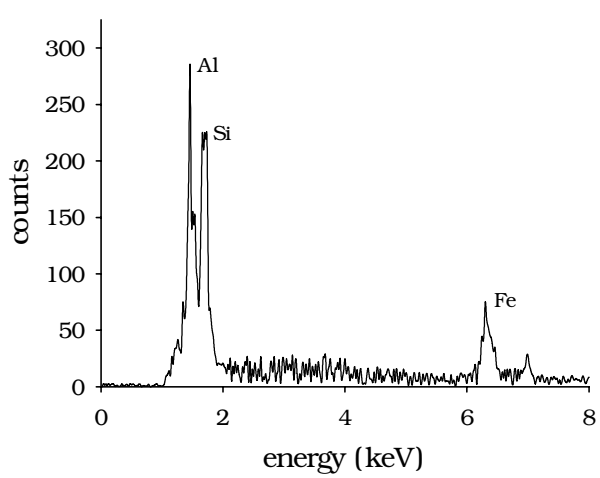

(c)

Figure 2. Electron microprobe images of resin-impregnated thin section of contaminated zone sediments of the Cape Cod glacial outwash aquifer showing Al-, Si-, and Fe-rich coating on quartz grain at two different scales: **(a)** scale bar, 100µm; magnification, 55 times; **(b)** scale bar, 10 µm, magnification 500 times. Dark grains are quartz; bright rims contain Al, Si, and Fe. EDX scan of coating **(c)**.

Table 8. Aquifer sediment zeta potentials under ambient and perturbed conditions.

sample	conditions	zeta potential (mV)
uncontam sediment in uncontam groundwater	ambient, pH 5.8	-22±1
	1 mM NaBr	-23±1
	72 µM NaDBS	-30±1
	49 mM NaDBS	-43±1
	pH 10.0	-30±1
	pH 11.0	-31±2
contam sediment in contam groundwater	ambient, pH 6.2	-27±1
	1 mM NaBr	-27±1
	72 µM NaDBS	-24±1
	49 mM NaDBS	-40±1
	pH 10.0	-31±1
	pH 11.0	-35±1

Table 9. Natural colloid zeta potentials under ambient and perturbed conditions.

sample	conditions		zeta potential (mV)
natural colloids mobilized from uncontam sediments suspended in deionized water	pH	2.3	0±8
		2.9	-4±2
		3.7	-18±5
		5.6	-26±3
		6.2	-33±4
		7.8	-37±3
		8.8	-44±2
		10.1	-43±4
		11.4	-42±7
		12.0	-45±8
natural colloids mobilized from uncontam sediments pH 5.8	NaDBS	0	-28±6
		0.57 mM	-27±2
		2.9 mM	-33±5
		14 mM	-45±6
		29 mM	-46±4

During the 1996 experiment, NaDBS was more effective at mobilizing colloids and viruses in the contaminated zone than in the uncontaminated zone. A comparable experiment was not carried out during the 1997 field season. SEM examination of filtered particles revealed at least 90% silica colloids; therefore, no correction for mobilization of natural colloids was applied. The migration of the surfactant closely matched the tracer migration. The mobilized colloids and viruses appeared at the first MLS concurrently or slightly behind the surfactant peak concentration.

During the 1996 experiment, ascorbic acid was more effective at mobilizing the silica colloids than the viruses. A comparable experiment was not conducted during the 1997 field season. SEM examination of filtered particles revealed at least 90% silica colloids; therefore, no correction for mobilization of natural colloids was applied. The transport of ascorbic acid was attenuated, especially in the uncontaminated zone, but no significant retardation of ascorbic acid occurred. The mobilized colloids and viruses appeared at about the same time or slightly after the appearance of the ascorbic acid peaks at the first MLS. The ascorbic acid injection produced a significant increase in the Fe(II) concentration in the contaminated zone, but no significant increase above the detection limit in the uncontaminated zone. Dissolved oxygen concentrations were slightly depressed in the uncontaminated zone during the ascorbic acid injection, but not significantly different in the contaminated zone.

During the 1997 experiments, a decrease in ionic strength brought about by an injection of 100 L of deionized water mobilized more colloids in the uncontaminated zone of the aquifer. The mobilized colloids appeared at the 1 m transport distance at the same time or slightly behind the deionized water pulse.

Discussion

Silica and Silica-Coated Colloid, PRD1, and Aquifer Grain Zeta Potentials During Injections. The negative zeta potentials of the silica and silica-coated colloids reflect the predominance of deprotonated surface hydroxyls at pH values above the pH_{pzc}

Table 10. Amount of natural colloids mobilized by chemical perturbation injections.

experiment	conditions	aquifer zone	mass of colloids mobilized[a] (mg)
elevated pH (NaOH)	11	uncontam	0.75
		contam	0.45
	12.5	uncontam	500
		contam	17
elevated surfactant NaDBS	0.57 mM	uncontam	59
		contam	20
	29 mM	uncontam	n.r.
		contam	n.r.
elevated reductant AscAc	1.0 mM	uncontam	41
		contam	2.0
decreased ionic strength deionized water	<5 µS cm-1	uncontam	2.7
		contam	1.1

[a] *Mass of colloids mobilized over the first meter of transport.*
[b] *No significant increase in turbidity occurred during the pH 10 injections.*
[c] *n.r.: not reported owing to interference in turbidity measurements by bubbles.*

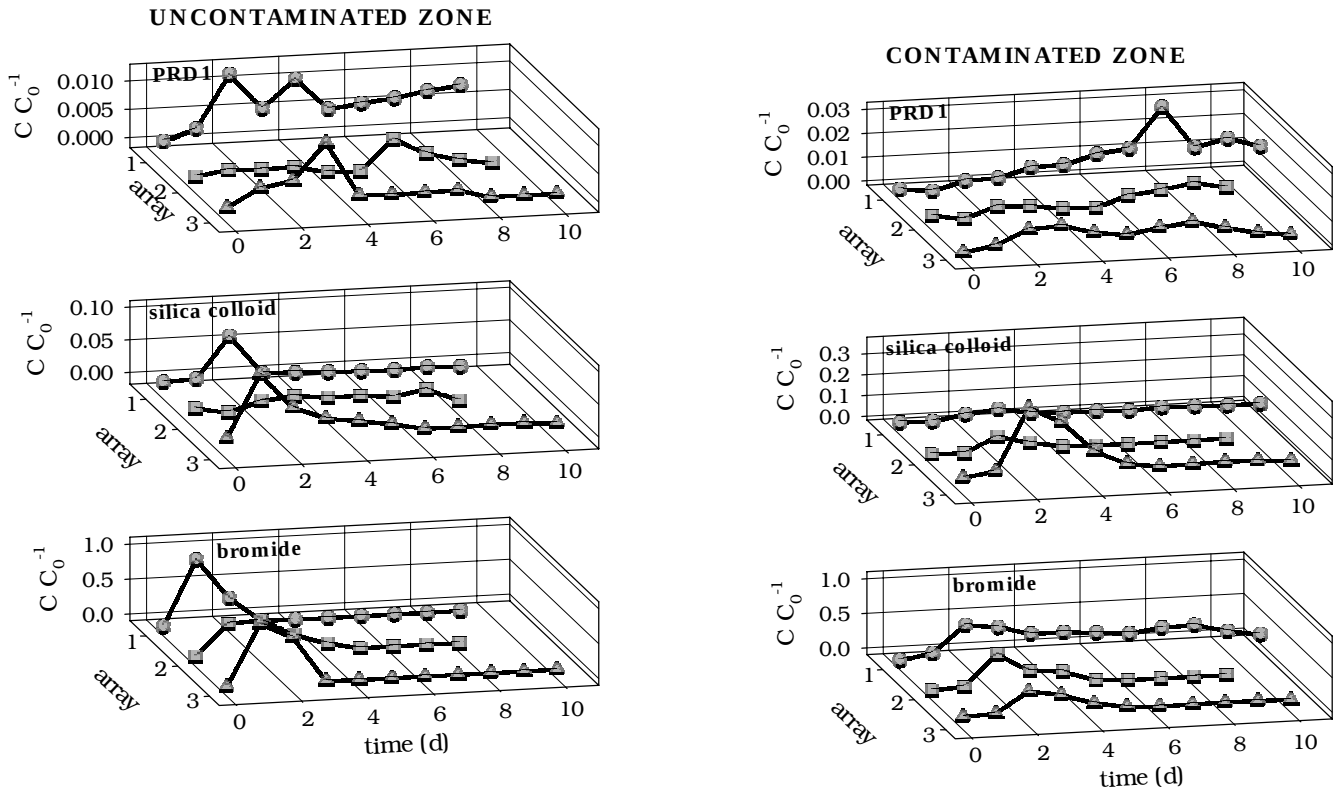

Figure 3. Silica colloid, bacteriophage PRD1, and bromide breakthrough curves at 1 m transport distance from 1996 deposition experiment in (a) uncontaminated and (b) contaminated zones of Cape Cod aquifer. Colloid, virus, and tracer concentrations (C) are normalized to their concentration immediately after injection (C_0).

Table 11. Summary of relative breakthroughs (*RB*) and collision efficiencies (α) calculated with and without dispersion for silica and silica-coated colloids and PRD1.

colloid	aquifer zone	replicate arrays	*RB* (%)	α with dispersion
PRD1	uncontam	3	2.5±1.7	0.032±0.016
	contam	3	4.3±1.4	0.016±0.005
silica	uncontam	3	13±4	0.023±0.009
	contam	3	37±16	0.0056±0.0034
silica-coated ZrO_2	uncontam	3	1.3±1.5	0.039±0.013
	contam	3	34±42	0.012±0.008
silica-coated ZrO_2 after 1% NaDBS	uncontam	1	78	0.0021
	contam	1	76	0.0017
silica-coated TiO_2 after 1% NaDBS	uncontam	1	11	0.0077
	contam	1	12	0.0090

Table 12. Recovery of silica and silica-coated colloids and PRD1 over the first meter of transport. Two pairs of recoveries are listed for the silica colloids at an elevated pH of 12.5 – the first pair is for silica colloids measured by UV absorbance and the second pair is for silica colloids measured as 0.6 times the sample turbidity to account for natural colloids.

chemical perturbation	conditions	colloid	aquifer zone	recovery (%)
elevated pH NaOH	10.0	silica-coated ZrO_2	uncontam	0.00
			contam	0.10
	11.0	silica-coated ZrO_2	uncontam	1.5
			contam	0.70
	12.5	PRD1	uncontam	100
			contam	78
		silica (UV)	uncontam	240
			contam	120
		silica (0.6 turb)	uncontam	103
			contam	37
elevated surfactant NaDBS	0.57 mM	PRD1	uncontam	0.5
			contam	49
		silica (UV)	uncontam	3.5
			contam	15
elevated reductant AscAc	1.0 mM	PRD1	uncontam	3.8
			contam	24
		silica (UV)	uncontam	51
			contam	27
decreased ionic strength deionized water	<5 μS cm^{-1}	silica-coated ZrO_2	uncontam	0.50
			contam	0.10

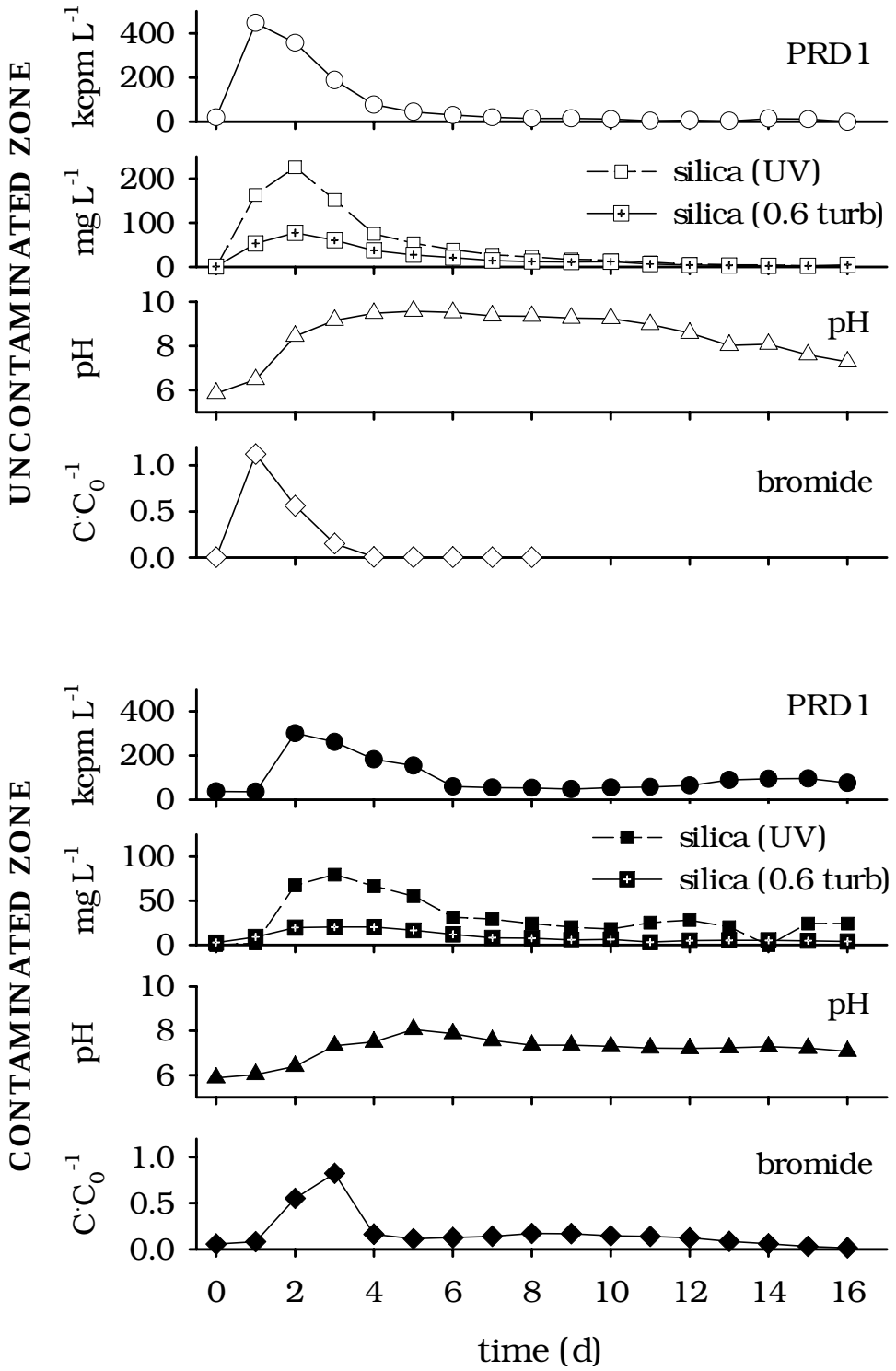

Figure 4. Mobilization of silica-coated zirconia colloids after deposition by elevation of pH (pH 11) at 1 m transport distance during 1997 field experiments. Silica-coated zirconia colloids measured as Zr by ICP-AES. Bromide tracer breakthrough presented as normalized concentration.

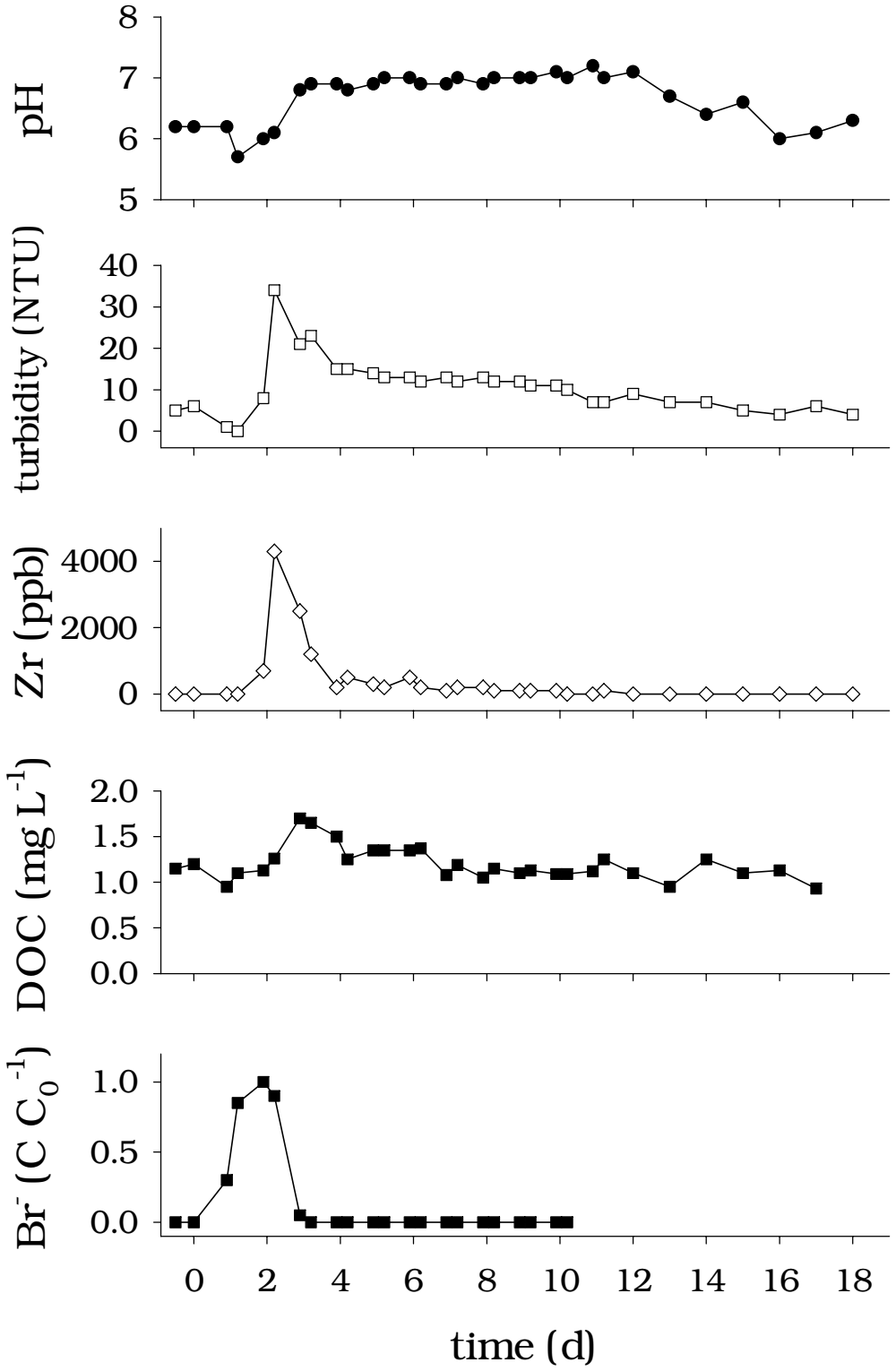

Figure 5. Mobilization of silica-coated zirconia particles by an increase in pH in the uncontaminated zone during the 1997 field experiments. The breakthrough of zirconium, turbidity, and dissolved organic carbon (DOC) slightly precede the advance of the pH increase.

value of about 2 to 2.5 reported for silica [Parks, 1965]. The similarity between the pH_{pzc} and the zeta potentials of the silica and silica-coated colloids indicate that the silica coating thickness of 10 to 60 nm was sufficient to mask the underlying surface properties of zirconia and titania.

The pH_{pzc} for PRD1 in the uncontaminated groundwater is less than 3.2, similar to a pH_{pzc} value of less than 3.9 in a calcium phosphate solution. On the basis of studies by Penrod et al. [1996] relating the pH_{pzc} values of bacteriophage MS2 and lambda to the composition of their protein capsids, these low pH_{pzc} values for PRD1 indicate that deprotonated carboxyl groups in amino acids dominate the surface speciation of the PRD1 protein capsid.

In the contaminated groundwater, the silica and silica-coated colloids and PRD1 were slightly more negative than in the uncontaminated groundwater. For PRD1, the change in zeta potential may simply be caused by the higher pH of the contaminated groundwater, although changes in virus surface charge may also be attributed to surfactants [Small and Moore, 1987] and fulvic acid [Bixby and O'Brien, 1979]. The silica colloids, however, appear to have reached a constant zeta potential at about pH 4.4, so the more negative zeta potential measured in the contaminated groundwater cannot be attributed to the higher pH of the contaminated groundwater. The zeta potential of the silica colloids must have been made more negative by adsorption of anions; e.g., organic matter and phosphate. While extensive adsorption of organic matter to silica at pH near 6.0 is unlikely owing to electrostatic repulsion [Davis, 1982], calcium and magnesium in the contaminated groundwater may enhance organic matter adsorption by reducing the negative charge of the organic matter.

The measured zeta potentials of the aquifer grains represents the net charge of a heterogeneous surface made up of the underlying quartz grains, ferric oxyhydroxide and clay mineral coatings, and adsorbed organic matter and phosphate. At the ambient pH of the groundwater, quartz is negatively charged, ferric oxyhydroxide is positively charged, and clay minerals are negatively charged overall with positively charged edges [Parks, 1967]. Adsorption of organic matter and phosphate to the positively charged surfaces reverses the surface charge [Liang and Morgan, 1990]. The net negative surface potential of the uncontaminated sediment suggests that the ferric oxyhydroxide coating on the quartz grains is patchy, as suggested by thin sections of Cape Cod aquifer grains examined by Coston et al. [1995] and this study (Figure 2). We attribute the more negative zeta potential of the contaminated sediment to the much higher organic matter content of the contaminated sediments (Table 1). The phosphate content of the contaminated sediments is also elevated, but only by a maximum factor of about 2.5.

Silica and Silica-Coated Colloid and PRD1 Deposition Behavior. Most studies of virus attachment to mineral grains conclude that electrostatic forces dominate the interaction between virus and grain surfaces [Gerba, 1984; Murray and Parks, 1980; Loveland et al., 1996; Penrod et al., 1996; Redman et al., 1997]. If electrostatic forces dominated colloid and virus deposition in these experiments, the zeta potential data should provide a qualitative explanation for the observed deposition behavior.

Both the silica and silica-coated colloids and viruses were transported through the contaminated zone more readily than through the uncontaminated zone. The greater abundance of organic matter in the contaminated sediments appears to have masked the ferric oxyhydroxide coatings, giving the contaminated sediments a greater negative zeta potential than the uncontaminated sediments. Consequently, when the negatively charged colloids and viruses interact with the contaminated sediments, they experience greater repulsion, resulting in collision efficiencies lower than those measured in the uncontaminated zone.

The zeta potential data and the ferric oxyhydroxide coatings detected in the thin sections indicate that ferric oxyhydroxides in the Cape Cod sediments enhance colloid and virus attachment and organic matter in the sewage plume inhibits colloid and virus attachment. The presence of positively charged oxides limits the transport of viruses and bacteria because these "biocolloids" are typically negatively charged at the ambient pH of most waters and readily attach to positively charged surfaces [Murray and Parks, 1980; Moore et al., 1981; Farrah and Preston, 1991; Scholl and Harvey, 1992; Mills et al., 1994; Loveland et al., 1996]. For mineral colloids, Johnson et al. [1996] showed that the transport of silica colloids in a porous media consisting of mixtures of clean and iron oxide-coated quartz sand depends strongly on the amount of iron oxide coating. Organic matter of natural and anthropogenic (e.g., sewage, surfactants) origin hinders virus attachment to mineral surfaces [Charney et al., 1962; Burge and Enkiri, 1978; Sobsey et al., 1980; Gerba et al., 1981; Moore et al., 1981; 1982; Atherton and Bell, 1983; Fuhs et al., 1985], presumably by adsorbing to and masking virus attachment sites. Similarly, the transport of ferric oxide colloids is enhanced by natural organic matter in quartz sands [Amirbahman and Olson 1993; Kretzschmar et al., 1995].

The differences between silica and silica-coated colloid and virus deposition are more subtle and not statistically significant, but a qualitative explanation of their deposition behavior based on the presence of ferric oxyhydroxide coatings and measured zeta potentials fits the trend of the mean collision efficiencies measured in the experiments. In both groundwaters, the silica and silica-coated colloids possess slightly greater negative zeta potentials, resulting in lower overall collision efficiencies. The close dependence of the measured collision efficiencies on the zeta potentials of the PRD1, silica colloids, and aquifer grains reinforces the conclusion that electrostatic forces dominate the transport behavior of viruses in porous media.

In one 1997 experiment, the transport of silica-coated zirconia and titania colloids was measured in a simultaneous injection with dodecylbenzene sulfonate. The collision efficiency calculated for the silica-coated titania particles was about 4-5 times greater than that calculated for the silica-coated zirconia particles (Table 11), indicating greater repulsion between colloid and grain for the silica-coated titania particles. This result qualitatively agrees with the zeta potentials measured for the two colloids – the silica-coated titania colloids have greater negative zeta potentials than the silica-coated zirconia colloids near the ambient pH of the groundwater (Tables 5,6).

Grain Surface Heterogeneity and Collision Efficiencies. The aquifer grain surfaces are primarily made up of patchy coatings of ferric oxyhydroxides on the underlying quartz grains. At the ambient pH of the groundwaters, the negatively charged PRD1 should be collected by the ferric oxyhydroxide coating and repelled by the exposed quartz [Loveland et al., 1996]. The measured collision efficiencies should reflect the summed contribution of ferric oxyhydroxide and quartz surfaces [Song et al., 1994; Johnson et al., 1996]. Using PRD1 collision efficiencies of $\alpha_{FeOx} \approx 1$ for ferric oxyhydroxide (owing to electrostatic attraction) and $\alpha_{qtz} \approx 6\times10^{-3}$ for quartz surfaces [Bales et al., 1991], we can

estimate the fraction of the surface area coated by ferric oxyhydroxide, f_{FeOx}, using the following equation:

$$\alpha_{measured} = f_{FeOx}\ \alpha_{FeOx} + f_{qtz}\ \alpha_{qtz} \quad (1)$$

This equation gives estimates of f_{FeOx} = 0.026 for the uncontaminated zone and f_{FeOx} = 0.010 for the contaminated zone. The uncontaminated zone f_{FeOx} estimate is in close agreement with the 3.0% surface coverage detected by electron microprobe in the thin sections, but the contaminated zone f_{FeOx} estimate is lower than the 3.5% surface coverage detected. No significant difference between the surface coverage in the uncontaminated and contaminated zones was observed in the thin sections; therefore, the lower contaminated zone f_{FeOx} estimate is attributable to the masking of ferric oxyhydroxide coatings by organic matter and phosphate adsorption.

Colloid and Virus Mobilization by Elevated pH. The NaOH injection was designed to reverse the charge on the ferric oxyhydroxide coatings by raising pH above the pH_{pzc} of ferric oxyhydroxides [Parks, 1967]. The amount of colloid and PRD1 mobilization increased with increasing pH. Although the precision of the silica colloid recovery measurement is clouded by the presence of the natural colloids, it appears that similar amounts of PRD1 and silica colloids were released and that release occurred more readily in the uncontaminated zone.

In the uncontaminated zone, the lack of buffering in the groundwater and sediments resulted in a greater increase in pH and greater release of PRD1 and silica colloids than in the contaminated zone. The pH in the uncontaminated zone peaked at nearly 10 at the 1-m distance (injection pH 11.7), while the pH in the contaminated zone peaked at only 8.5 at the 1-m distance (injection pH 11.5) (Figure 4). An increase of pH to 10 is sufficient to reverse the surface charge of any ferric oxyhydroxide, but an increase to pH 8.5 may not exceed the pH_{pzc} of some ferric oxyhydroxides. The greater release of colloids and viruses in the uncontaminated zone must be attributed to the increase in pH well in excess of the pH_{pzc} of the ferric oxyhydroxide coatings.

In the contaminated zone of the Cape Cod aquifer, Bales et al. [1995] found that injection of a pH 8.3 solution containing an unspecified concentration of phosphate for buffering effectively re-mobilized PRD1 (a fractional recovery was not measured). This injection caused the detachment of PRD1 even when the pH increase down-gradient of the injection was only slightly above the ambient pH. It is likely that the phosphate augmented the charge reversal caused by the pH increase by adsorbing to the ferric oxyhydroxide coatings.

Colloid and Virus Mobilization by Surfactant Addition. NaDBS was added to alter the ferric oxyhydroxide surface charge and promote release. NaDBS is an anionic surfactant that readily adsorbs to positively charged oxide surfaces and reverses surface charge by hemimicelle formation [Dick et al., 1971]. Similar surfactants have been shown to mobilize natural colloids [Ryan and Gschwend, 1994] and cause permeability reduction through colloid mobilization [Allred and Brown, 1994]. The high NaDBS injection concentration made it difficult to determine with any precision the amount of NaDBS lost to aquifer sediments by adsorption. Only a small fraction of the NaDBS injected would be required to saturate the ferric oxyhydroxide surfaces with adsorbed NaDBS [Pieper et al., 1997]; however, NaDBS was much less effective at mobilizing PRD1 and silica colloids than the increase in pH. Similarly, Bales et al. [1991] showed that 1% Tween 80 and 2.5% beef extract solutions were only marginally effective at mobilizing PRD1 and MS2, another bacteriophage, relative to an increase in pH to 8 in a sodium phosphate solution. Bales et al. [1991] speculated that the high ionic strength of the surfactant and beef extract solutions inhibited virus detachment. Our addition of NaDBS to the Cape Cod groundwater caused an increase in ionic strength (0.57 mM) less than that caused by the sodium bromide tracer (about 1.5 mM).

NaDBS was much more effective at mobilizing PRD1 and silica colloids in the contaminated zone. In a previous experiment, Pieper et al. [1997] similarly observed that a 25 mg L^{-1} mixture of linear alkylbenzenesulfonates (LAS) recovered 87% of the injected PRD1 in the contaminated zone and only 2% in the uncontaminated zone. The abundance of organic matter in the contaminated zone must reduce the amount of surfactant needed to reverse the charge of ferric oxyhydroxide surfaces. In this experiment, the higher concentration of NaDBS (0.57 mM; 200 mg L^{-1}) did not improve recovery. The results suggest that PRD1 and silica colloids are more strongly bound in the uncontaminated zone.

Colloid and Virus Mobilization by Reductant Addition. Ascorbic acid was added to remove the ferric oxyhydroxide coatings by reductive dissolution, resulting in the release of PRD1 and silica colloids attached to the coatings. Ryan and Gschwend [1994] observed that reductive dissolution by ascorbate mobilized natural colloids from a similar ferric oxyhydroxide-coated quartz sand as long as increases in the ascorbate concentration did not raise ionic strength to a level too high to inhibit release. In this experiment, ascorbic acid addition promoted PRD1 and silica colloid release that was somewhat comparable to the surfactant addition, but less than that caused by the pH increase. The amount of ascorbic acid injected in this experiment was similar to the amount promoting the maximum colloid release in the experiments of Ryan and Gschwend [1994].

The amount of PRD1 and silica colloid release varied inconsistently in these experiments. Ascorbic acid appeared to be effectively dissolving ferric oxyhydroxides in the contaminated zone because the Fe(II) concentration increased as the ascorbic acid broke through; however, Fe(II) release continued near the peak level of Fe(II) release for 15 days beyond the ascorbic acid breakthrough. In contrast, very little ascorbic acid broke through and very little Fe(II) was released in the uncontaminated zone. Some ascorbic acid may have been oxidized by oxygen, although no significant changes in the oxygen content were observed. Released Fe(II) may have been re-adsorbed by aquifer grains or by released colloids, in which case the Fe(II) would promote destabilization and deposition. Based on these results, it is difficult to assess the dependence of PRD1 and silica colloid recovery by ascorbic acid addition.

Colloid Mobilization by Ionic Strength Decrease. Decreases in groundwater ionic strength have frequently caused substantial colloid mobilization and permeability reduction during artificial recharge [Nightingale and Bianchi, 1977] and secondary oil recovery [Khilar and Fogler, 1984]. When low ionic strength water replaces high ionic strength water in aquifers with substantial clay contents, an expansion of double layers leads to an increase in electrostatic repulsion between colloids and grains and colloid mobilization. In the ferric oxyhydroxide-coated sands at Cape Cod, however, we hypothesized that a decrease in ionic strength would not cause substantial colloid mobilization because most of the colloid-grain interaction is attractive (negatively charged colloids, positively charged grain coatings). A decrease in ionic

strength and expansion of double layers would only serve to strengthen this attractive interaction. As hypothesized, the decrease in ionic strength caused minimal mobilization of the natural colloids and the silica-coated zirconia colloids. There was one exception – when the deionized water pulse followed the 0.1 M calcium chloride pulse, a substantial recovery of the silica-coated zirconia was observed. In this extreme case, we surmise that colloids were mobilized where they were bound to bare quartz surfaces. No mobilization occurred without the calcium chloride pulse preceding the deionized water pulse because the contrast in ionic strength was not sufficient.

Laboratory Experiments

Purpose

To address one of the overall objectives of the project, to examine the dependence of colloid transport and mobilization on chemical perturbations, a set of laboratory experiments were conducted to assess the rate of natural colloid mobilization from the ferric oxyhydroxide-coated quartz sands from Cape Cod under more controlled conditions. These laboratory experiments included the following tests:

- measurement of colloid mobilization in the laboratory from undisturbed, oriented sediment samples;
- quantitation of the rate of colloid mobilization under controlled conditions; and,
- examination of a range of chemical perturbations wider than possible in the field to understand the dependence of the amount and rate of colloid mobilization on the chemical conditions.

To perform these experiments, we developed a special column packing technique to load the Cape Cod sediments into a column with a minimum of disturbance to the grain-grain arrangement. We then subjected these packed columns to a wide range of chemical perturbations and measured colloid mobilization using flow-through meters and a data acquisition system.

Materials and Methods

Sediment Characterization. Experiments were conducted on uncontaminated and contaminated sediment samples from the U.S. Geological Survey's Cape Cod field site. To confirm the location of the sewage plume in the sediment cores, pore waters were displaced with nitrogen pressure from the cores and measured pH, specific conductance, and dissolved oxygen. Owing to some unavoidable atmospheric contact, specific conductance was the best measure of contamination. Cores with a specific conductance of less than 100 S cm^{-1} were identified as uncontaminated and cores with a specific conductance of greater than 300 S cm^{-1} were identified as contaminated. Cores of intermediate specific conductance were not used in the laboratory experiments.

Column Packing and Setup. To prepare undisturbed, oriented sediment columns, a stainless steel column (5.0 cm length, 2.5 cm diameter) was gently rotated into a sediment core through a hole drilled horizontally in the acrylic core sleeve. From a hole drilled on the opposite side of the core, the sediments were lightly pressed into the column using a plunger of 2.5 cm diameter [Ard, 1997]. The sediment was secured in the column by threaded stainless steel caps, Teflon® washers, a 0.2 μm stainless steel frit on the influent end (bottom), and a 105 μm polypropylene mesh on the effluent end (top). The dry weight of sediment packed into the column averaged 38.6±2.0 g. The average column porosity was 0.41±0.02 assuming a sediment grain density equal to that of quartz (2.65 g cm^{-3}). The average column pore volume, 9.0±0.5 mL, was measured by the decrease in mass after removing water from a saturated column and drying at 105°C overnight.

Influent solutions were pumped through the column at a flow rate of 0.15 mL min^{-1} (representing an interstitial groundwater velocity of 0.7 m d^{-1}) using syringe pumps to ensure constant surge-free flow. The column effluent flowed through (1) micro-cells measuring specific conductance and pH (volumes of 17 and 11μL, respectively) and (2) a turbidity cell (volume about 2 mL) to a fraction collector. A data acquisition system was used to record data at 1 min intervals.

Column Procedures. After packing each column, the sediment was flushed with a high ionic strength solution (0.5 M NaCl) to remove colloids loosened by column packing until a low background turbidity (roughly 5 NTU) was observed (typically 5 pore volumes). Next, a low ionic strength solution (5.0×10^{-4} M NaCl) representative of the ionic strength of the uncontaminated groundwater, was run through the column until a low baseline turbidity (roughly 5 NTU) and specific conductance was observed (typically 25 pore volumes).

The sediments were subjected to a series of chemical perturbations that enveloped those tested in the field experiments. In some experiments, a single sediment column was subjected to a sequence of chemical perturbations (Table 13). In these experiments, each influent solution was separated by a "groundwater flush" of 5.0×10^{-4} M NaCl run until the turbidity in the effluent returned to the background level. In other experiments, a series of individual columns were subjected to a series of chemical perturbations (Table 14). The surfactant concentration perturbations ranged from one-tenth the value of the critical micelle concentration (CMC) for sodium dodecylbenzene-sulfonate, 1.2 mM [Mukerjee and Mysels, 1971], to approximately ten times the CMC in a 5% solution.

Colloid Characterization. The elemental composition, morphology, mineralogy, and zeta potential of the natural colloids were characterized as described in the field experiments. The total mass of mobilized colloids was determined by integrating the colloid concentration in the column effluent over the time of release and multiplying this by the flow rate. This method assumes deposition of mobilized colloids is negligible.

Results

Colloid Characterization. The elemental and mineral composition, morphology, and zeta potentials of the mobilized colloids closely matched those of the colloids mobilized in the field experiments. No significant differences were observed between colloids mobilized by different water chemistries.

Sequential Perturbation Experiments. The sequential pH increase experiments revealed that very little colloid mobilization occurred until the influent pH solution reached pH 9.5 and 10.5. Only the two highest NaDBS concentrations caused significant colloid release. The ascorbic acid injections caused the most release during the intervening groundwater flushes.

At the highest colloid mobilization rates by all three perturbations, it became apparent that the sequential perturbations were removing too many colloids for the later perturbations to accurately measure the rate and amount of colloid mobilization. We were able to compare the total amount of colloids mobilized to assess the contrast between the uncontaminated and contaminated sediments (Table 15). During pH increase sequence, about twice as many colloids were mobilized from the contaminated sediment as in the uncontaminated sediment (in contrast to the field experiments). During the NaDBS increase sequence, about 7 times as many colloids were mobilized in the contaminated sediment as in the uncontaminated sediment (in agreement with the field experiments). During the ascorbic acid

Table 13. Influent solutions for the sequential column colloid mobilization experiments on uncontaminated and contaminated sediments. Each of these influent solutions was followed by flushing by a "groundwater" solution of $5x10^{-4}$ M NaCl (pH 6 and conductivity 70 µS cm^{-1}).

perturbation	constituents	unit	sequence of perturbations					
elevated pH (NaOH)	pH		5.5	7.5	9.5	10.5	11.5	12.5
	NaBr	mM	1.5	1.5	1.5	1.5	1.5	1.5
	conductivity	mS cm^{-1}	0.20	0.20	0.20	0.25	1.0	10
elevated surfactant (NaDBS)	NaDBS	mM	0.12	0.60	1.2	29	140	
	NaBr	mM	1.5	1.5	1.5	1.5	1.5	
	conductivity	mS cm^{-1}	0.20	0.20	0.35	1.5	6.5	
elevated reductant (AscAc)	AscAc	M	0.0001	0.001	0.01	0.1		
	NaBr	mM	1.5	1.5	1.5	1.5		
	conductivity	mS cm^{-1}	0.20	0.25	0.80	6.0		

Table 14. Influent solutions for the individual column colloid mobilization experiments on uncontaminated sediment.

perturbation	constituents	unit	sequence of perturbations			
elevated pH (NaOH)	pH		10.5	11.5	12.5	13.1
	NaBr	mM	1.5	1.5	1.5	1.5
	conductivity	mS cm^{-1}	0.25	1.0	10	80

Table 15. Total mass of natural colloids mobilized from the uncontaminated and contaminated Cape Cod sediments by sequential chemical perturbations. The mass of colloids mobilized in the pH and NaDBS experiments was calculated as the sum of colloids mobilized only during the chemical perturbation steps. For the AscAc experiment, the mass of colloids mobilized also included the colloids mobilized during the intervening groundwater flushing steps.

perturbation	aquifer zone	mass of colloids mobilized (mg)
elevated pH NaOH	uncontam	3.4
	contam	7.2
elevated surfactant NaDBS	uncontam	0.14
	contam	1.0
elevated reductant AscAc	uncontam	0.47
	contam	0.89

increase sequence, about twice as many colloids were mobilized in the contaminated sediment as in the uncontaminated sediment (in agreement with the field experiments).

Individual pH Increase Experiments. The amount of colloids mobilized from the individual columns increased with increasing pH up to pH 12.5, and then decreased substantially at pH 13.1 (Table 16; Figure 6). The pH 10.5 influent produced a long, slow colloid release that lasted about 120 pore volumes before returning to the background turbidity level. The pH 11.5 influent produced greater and more rapid colloid release than pH 10.5; only about 25 pore volumes were required for return to background turbidity. Colloid release at pH 12.5 influent was even greater and more rapid than the lower pH influents. The pH 13.1 influent produced the most rapid colloid release, but the total mass of colloids released was small. Details of this experiment will be described in Ryan, Ard, Magelky, and Elimelech [in preparation].

Discussion

Colloid-Grain Morphology and Composition. The sediments at the Cape Cod site are primarily composed of iron oxyhydroxide-coated quartz [Coston et al., 1995]. At the ambient pH of the groundwater (5.4 to 6.0), quartz is negatively charged (pH_{pzc} of approximately 2.0 [Parks, 1967]). The colloids, mainly clay particles, also possess net negative charge at this pH value. Any ferric oxyhydroxides present in the coatings, however, are positively charged at the ambient pH (e.g., hematite, pH_{pzc} 6.7; goethite, pH_{pzc} 8.5; lepidocrocite, pH_{pzc} 7.4 [Parks, 1967]). On the basis of these surface properties, it is likely that the ferric oxyhydroxide coatings act as a cementing layer between the grains and colloids. Ryan and Gschwend [1990] made the same argument for ferric oxyhydroxide-coated quartz sands in two Atlantic Coastal Plain sediments.

Effect of pH on Colloid Mobilization. Substantial colloid mobilization began to occur at pH 9.5, but not at pH 7.5. This threshold appears to represent the pH at which the surface charge of the ferric oxyhydroxide cement was reversed from positive to negative. At pH 9.5, all of the mineral components of the system become negatively charged and colloid release occurs. Ryan and Gschwend [1994] observed colloid release threshold at a similar pH value during colloid release experiments in a ferric oxyhydroxide-coated quartz sand from the Cohansey Formation in New Jersey.

As the influent pH was increased to 10.5, 11.5, and 12.5, the rate and total mass of colloid release increased. The increase in pH increased the negative zeta potentials on the colloid and grain surfaces. The increased negative zeta potentials caused greater colloid-grain repulsion. Relating the rate and amount of colloid release to the amount of repulsion is challenging for natural systems, but we have observed a clear relationship here between the rate and extent of colloid mobilization and the colloid and grain surface charge.

Increasing the influent pH to 13.1, however, substantially decreased the amount of colloid release, while the rate of release remained rapid. Similar colloid release behavior has been observed by Kolakowski and Matijevic [1979] in a model system of chromium hydroxide colloids and glass beads. During the transition from ambient pH to 13.1, the colloid and grain surfaces became increasingly repulsive; however, as the column effluent pH reached 13.1, the ionic strength exceeded 0.1 M. The high ionic strength compresses the repulsive double layers and shields the colloid and grain from repulsion; hence, colloid release was shut down. The initial pulse of colloid release was still rapid because the pH in the column was rapidly increasing to 13.1 through the pH range that promoted colloid release. At some pH value between 12.5 and 13.1, the colloid and grain surfaces have reached their maximum negative surface charge. The additional increase in pH is only raising ionic strength, not making the colloid-grain interactions more repulsive. Inhibition of colloid release by elevated ionic strength was also observed in the field. Although a large release of colloids was measured at the 1 m transport distance during the pH 12.5 injection, little release was observed at the injection point itself.

In contrast with the sequential pH increase experiments, the release of colloids in the uncontaminated zone was much greater than that in the contaminated zone during the individual column experiments. The individual column experiment results agree with the field experiments. Greater release in the uncontaminated zone can be attributed to its lower buffering capacity.

Sediment Disturbance and Orientation. Employing undisturbed and oriented samples for column experiments makes this laboratory work more applicable to in situ systems. Using disturbed Cape Cod sediments, Roy and Dzombak [1996] measured greater amounts of colloid release under similar chemical conditions. Disturbing the sediments through column packing can loosen attached colloids and destroy sediment arrangements that may have an effect on colloid mobilization. If repacking is avoided and columns are sampled without disturbance but the original orientation of the sediments is

Table 16. Results of the elevated pH colloid mobilization experiments for uncontaminated sediment in the individual column experiments.

pH	peak colloid concentration (mg L^{-1})	time of peak release (pore volume)	time to return to background (pore volume)	mass of colloids released (mg)
10.5	14.5	26	94	4.4
11.5	138	3.3	20	6.1
12.5	196	2.6	11	8.4
13.1	314	1.4	4.3	0.78

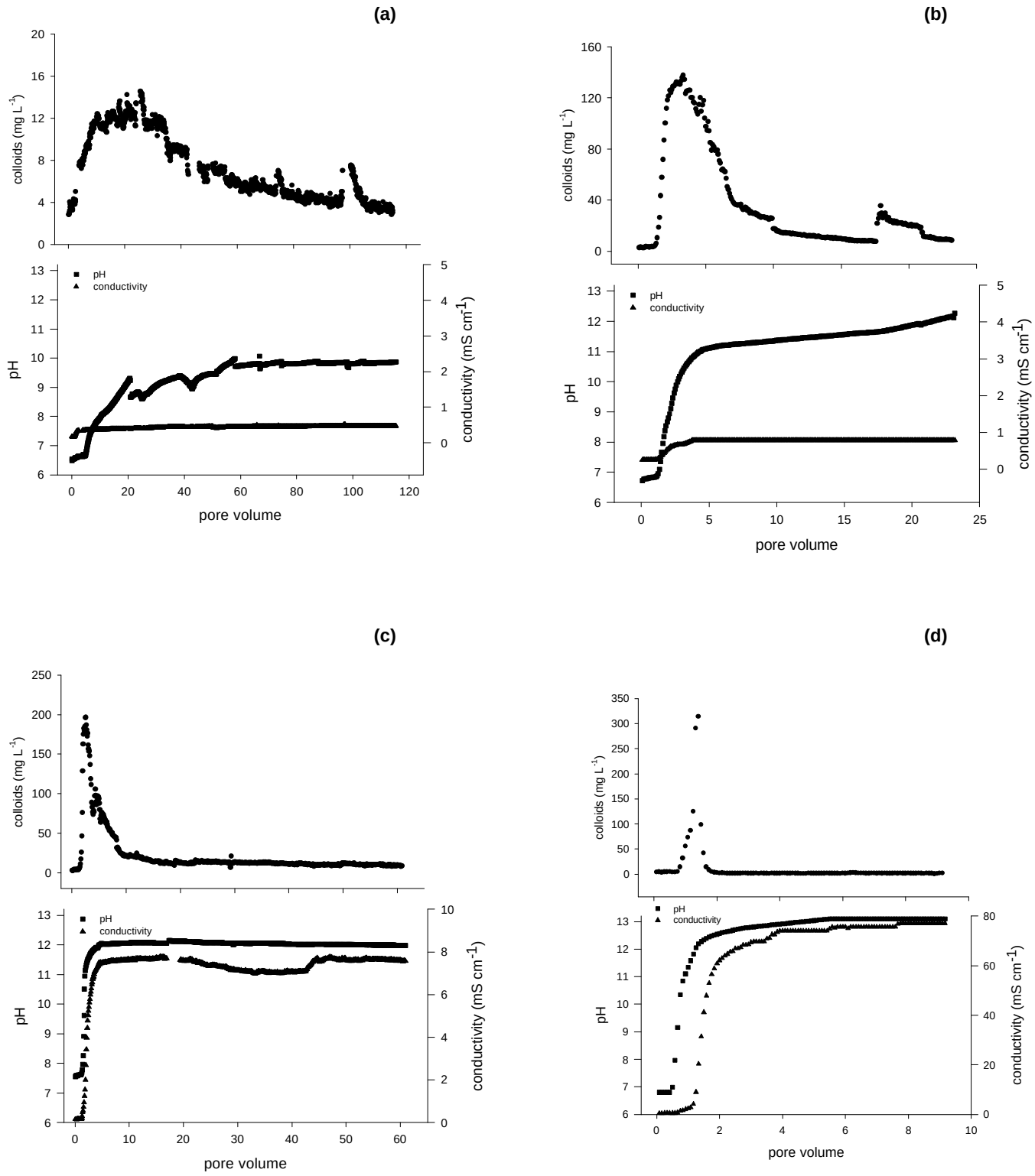

Figure 6. Natural colloid mobilization from oriented, undisturbed columns of uncontaminated sediment by pH elevation: (**a**) pH 10.5 influent, (**b**) pH 11.5 influent, (**c**) pH 12.5 influent, and (**d**) pH 13.1 influent.

changed, colloid mobilization results could still be very different from those witnessed in an in situ experiment. Sediment grains arrange themselves relative to the flow of groundwater around them, if the sediment orientation is ignored then an influent would be approaching the sediments at a different angle and towards a different sediment face than had previously been exposed to approaching groundwater. Though repacked and disoriented columns can help define colloid mobilization and transport trends, undisturbed and oriented columns will provide more applicable information.

Modeling

Purpose

To address the third of the major objectives of this project, the development of a colloid transport model that would describe the colloid transport in a contaminant plume, we undertook the modeling of colloid transport in a geochemically and physically heterogeneous porous medium similar to that found at the U.S. Geological Survey Cape Cod field site. As a first step toward modeling the effects of a contaminant plume on colloid transport, this model simulates the effect of heterogeneity and the dynamics of colloid deposition. The original objectives of developing a colloid transport model capable of simulating all of the processes playing a role in the transport of colloid in a contaminant plume were not met during this research period. Ongoing model development is still striving towards those original objectives.

Field and laboratory investigations on the transport of colloidal particles in aqueous porous media have demonstrated that advection, hydrodynamic dispersion, particle deposition, and particle release are the primary mechanisms controlling colloid transport in porous media [Harvey et al., 1989; Tobiason, 1989; Elimelech and O'Melia, 1990; Elimelech, 1991; Lindqvist and Enfield, 1992; Higgo et al., 1993; Harvey et al., 1995; Kretzschmar et al., 1995; Penrod et al., 1996; Harmand et al., 1996; Pieper et al., 1997]. Various models involving these four main colloid transport mechanisms have been developed based on colloid mass balance over a representative elementary volume (REV) of a porous medium. Among these four main colloid transport mechanisms, colloid deposition has been investigated more extensively.

The kinetics of particle deposition have been derived theoretically and measured experimentally. The theory of Derjaguin-Landau-Verwey-Overbeek (DLVO) was generally used to describe the surface-surface interactions to predict the particle deposition or release rates [Elimelech and O'Melia, 1990]. However, theoretical predictions are generally several orders of magnitude greater than experimental observations under unfavorable deposition conditions (i.e., when repulsive double layer interactions predominate). Various attempts have been made to explain this discrepancy, including attachment in secondary energy minima [McDowell-Boyer, 1992; Stumm and Morgan, 1995], interfacial dynamics of double layer interaction [Elimelech and O'Melia, 1990], and surface non-idealities [Song et al., 1994]. Among these explanations, geochemical heterogeneity (surface charge heterogeneity) is considered to be the most probable cause of the anomalous colloid deposition rates observed in porous media [Song et al., 1994].

The geochemical heterogeneity of granular porous media was modeled either as random microscopic sites or as patches [Song et al., 1994]. Patchwise charge heterogeneities are ubiquitous in subsurface environments due to geochemical variabilities inherent in mineral grains. Johnson et al. [1996] adopted the patch model to describe the geochemical heterogeneity of porous media. They assumed a constant geochemical heterogeneity for the entire porous medium and incorporated it into a colloid transport model.

The dynamics of colloid deposition have also been studied. A linear Langmuirian blocking function was proposed by Privman et al. [1991]. Song and Elimelech [1994] extended the model by including the non-uniform deposition resulting from spherical collector geometry and surface heterogeneities. The nonlinear random sequential adsorption (RSA) model was employed by Johnson and Elimelech [1995] to describe the dynamics of blocking in colloid deposition. More recently, Johnson et al. [1996] have incorporated the RSA model for dynamic blocking process and the patchwise model for geochemical heterogeneity into a colloid transport model. They found good agreement between model predictions and the experimental measurements.

There are relatively fewer theoretical formulations for colloid release, advection, and hydrodynamic dispersion. The colloid release is usually described as a kinetic process (first-order mechanism) instead of a dynamic process in colloid transport equation [Chrysikopoulos et al., 1990]. When the hydrodynamic chromatography effect is not obvious in colloid transport, the difference between the colloid advection velocity and the solute advection velocity (or colloid and solute dispersion coefficient) is usually ignored, and the hydrodynamic dispersion linearly depends on the advection velocity for both colloid and solute transport.

Most of the developed models only describe colloid transport in physically homogeneous porous media. However, porous media in subsurface environments are physically heterogeneous [LeBlanc, 1984; Hess et al., 1992]. Only Abdel-Salam and Chrysikopoulos [1995] modeled colloid transport in a fractured-rocks matrix using lognormally distributed fracture aperture. The physical heterogeneity was described as a random field. Saiers et al. [1994] carried out experiments of colloid transport in a structured-heterogeneous porous medium. In these experiments, the column was packed with different sand layers, which were parallel to the flow direction; each layer was packed homogeneously. This physical heterogeneity can be viewed as layered distributed. The results of both studies showed that physical heterogeneity of porous media can affect colloid transport significantly. These researchers focused on colloid advection and hydrodynamic dispersion to explain the consequences of the heterogeneous flow field on colloid transport. Although the flow velocity may also affect the kinetics of particle deposition or release, such effects were not considered in the above studies.

The previous modeling of colloid transport in geochemically heterogeneous porous media only dealt with the porous medium with a constant geochemical heterogeneity. However, a spatially distributed geochemical heterogeneity is very likely to exist in a porous medium due to the inherent variability of minerals. Thus, it is important to study the role of a spatial distribution of geochemical heterogeneity in colloid transport. Since geochemical heterogeneity has only recently been introduced to colloid transport studies, there have been no attempts to incorporate a distribution of geochemical heterogeneity into colloid transport modeling.

We developed a two-dimensional model for colloid transport in physically and geochemically heterogeneous porous media [Sun, Elimelech, Sun, and Ryan, submitted]. In this model, a patchwise geochemical heterogeneity and dynamic aspects of particle deposition and release are included in the governing equations for colloid transport, which are coupled with the flow equation.

Model Development

We consider a confined aquifer, where the fluid follows a steady laminar motion and the suspended colloidal particles

travel at the fluid velocity. The colloidal particles are assumed to be Brownian (i.e., less than about 1μm) and monodisperse. The steady state flow field is derived from the transient flow equation and incorporated into the colloid transport equation. Spatial distributions of the physical and geochemical heterogeneities of the subsurface porous medium are rigorously incorporated in the model.

Flow Field. The transient flow equation for a fluid in a confined subsurface porous medium, such as a confined groundwater aquifer, is usually written as

$$S_S \frac{\partial h}{\partial t} = \nabla \cdot (\mathbf{K} \cdot \nabla h) - Q \tag{2}$$

where h is the hydraulic head, t is the time, S_s is the specific storage, K is the hydraulic conductivity, and Q is the pumping or recharge rate. Under natural gradient flow conditions, colloid advection can be described by the steady-state flow equation. The spatially distributed hydraulic heads are used to calculate the velocity field by applying Darcy's law

$$\mathbf{q} = -\mathbf{K} \cdot \nabla h \tag{3}$$

where h is the hydraulic head gradient and $\mathbf{q}$ is Darcy's velocity. The average pore velocity (V), which is used in the colloid transport equation, is the ratio of Darcy's velocity to porosity.

Physical Heterogeneity of Subsurface Porous Media. The spatial variation of hydraulic conductivity is the principal cause of heterogeneous flow field that further influences colloid transport and the resulting particle concentration in the porous medium. Two types of physical heterogeneity are investigated, namely, layered heterogeneity and random heterogeneity.

In a layered, physically heterogeneous subsurface porous medium, the porous medium is made up of several homogeneous layers. Thus, while each layer is homogeneous (i.e., with constant hydraulic conductivity), the entire system is heterogeneous. Porous media with large blocks of macropores or fractures may be described as layered heterogeneous.

Substantial progress has been made in the past two decades to understand the random physical heterogeneity of groundwater aquifers. Evidence from field-scale hydraulic conductivity measurements indicates that the spatial distribution of hydraulic conductivity is lognormal [e.g., Freeze, 1975; Hoeksema and Kitanidis, 1984; Sudicky, 1986; Hess, 1989]. It was also found that there exists a non-Gaussian behavior of the log-transformed hydraulic conductivity at relatively small scales, and that this non-Gaussian behavior shifts to Gaussian behavior as the length scale increases [e.g., Painter, 1996; 1997; Liu and Molz, 1997]. Because of lack of knowledge on this transition length scale and the fact that lognormally distributed hydraulic conductivity has generally been used by numerous hydrologists [e.g., Gelhar et al., 1979; Gelhar and Axness, 1983; Dagan, 1984; Bellin et al., 1992], a lognormal distribution is adopted here to describe the random spatial variation of hydraulic conductivity.

Let $Y = ln\,\boldsymbol{K}$, with a constant mean m_Y and variance σ_Y^2. The covariance function of Y is assumed to have an isotropic exponential form,

$$C_Y(r) = \sigma_r^2 \exp\left(-\frac{|r_Y|}{l_Y}\right) \tag{4}$$

where r_Y is the planar distance vector between two positions in the heterogeneous domain and l_Y is the integral scale of Y. Using statistical properties of the spatial distribution, the random field of hydraulic conductivity can be generated by the turning band method [Mantoglou and Wilson, 1982; Tompson et al., 1989].

Geochemical Heterogeneity of Subsurface Porous Media. Coatings and patches of oxyhydroxides (iron and aluminum) on subsurface mineral grains are the main source of geochemical heterogeneity in groundwater aquifers [Coston et al., 1995; Ryan et al., 1999]. These coatings on mineral grain surfaces provide favorable sites (area) for colloid deposition. Here, we adopt the patch model [Song et al., 1994] to describe the geochemical heterogeneity of subsurface porous media. The model is characterized by the heterogeneity parameter, λ, which is defined as the ratio of the surface area favorable for colloid deposition to the total interstitial surface area over a REV of a porous medium. The surface area favorable for deposition is usually characterized by a surface charge opposite that of the colloids. Because most colloids are negatively charged, the favorable deposition areas are patches of positively charged minerals (e.g., iron and aluminum oxides, clay edges). Note that colloid deposition or release can occur on both the favorable and unfavorable fractions, albeit at much different rates.

Because the chemical composition of subsurface minerals and solution chemistry vary spatially in subsurface aquatic environments, the geochemical heterogeneity, defined over a REV, may vary significantly throughout the subsurface porous medium. The geochemical heterogeneity of a porous medium can be assumed to be constant over the entire porous medium, or to have different values at different locations in the porous medium. Accordingly, two spatial variations of geochemical heterogeneity are considered: layered geochemical heterogeneity and random geochemical heterogeneity.

Compared to layered geochemical heterogeneity, detailed statistical information on the chemical properties of the subsurface porous medium is needed to model random geochemical heterogeneity. To date, there are no reported studies on the random field of geochemical heterogeneity of subsurface porous media in relevance to colloid transport. Several studies on solute transport in heterogeneous porous media have described the variation of solute sorption coefficients by a normal distribution [e.g., Black and Freyberg, 1987; Chrysikopoulos et al., 1990; Bosma and van der Zee, 1993]. Although solute transport behavior is quite different than colloidal transport behavior, we adopt a similar approach and describe the random field of geochemical heterogeneity as normally distributed with a constant mean E(λ) and a variance σ_Y^2. The turning band method is used to construct the two-dimensional random field of normally distributed geochemical heterogeneity, with a first-order exponential autocorrelation function:

$$C_\lambda(r) = \sigma_\lambda^2 \exp\left(-\frac{|r_\lambda|}{l_\lambda}\right) \tag{5}$$

where l_λ is the integral scale of λ.

The average value of the geochemical heterogeneity parameter in groundwater aquifers is usually thought to be small, on the order of a few percent [Heron et al., 1994; Kretzschmar et al., 1995; Coston et al., 1995; Ryan et al., 1999]. With a mean value of only a few percent, normal distribution cannot cover a wide range of geochemical heterogeneity. Thus, in addition to normal distribution, a lognormal distribution will be used when significant variations of geochemical heterogeneity, with a small mean value of only a few percent, are desired.

Colloid Transport Equation. The colloid transport equation can be derived from mass balance of colloids over a REV of a porous medium. There are three main mechanisms controlling colloid transport: hydrodynamic dispersion, advection, and the colloid exchange between the stationary solid matrix and the mobile colloidal phase through colloid deposition and release. These mechanisms can be described by the generalized advection-dispersion equation [e.g., Corapcioglu and Kim, 1995]:

$$\frac{\partial C}{\partial t} = \nabla \cdot (D \cdot \nabla C) - \nabla \cdot (VC) - \frac{\rho_b}{\varepsilon} \frac{\partial S}{\partial t} \tag{6}$$

where C is the mass concentration of colloids in the aqueous phase, S is the ratio of the colloid mass captured by the solid matrix to the total mass of solid matrix, $\boldsymbol{D}$ is the particle hydrodynamic dispersion coefficient, $\boldsymbol{V}$ is the particle velocity, ε is the porosity of the porous medium, and ρ_b is the bulk density of the porous medium. Because the average pore radius in sandy aquifers is quite large compared to the size of Brownian (submicrometer-size) colloidal particles, size exclusion effects are not considered. Thus, the particle velocity and interstitial fluid velocity are assumed to be equal. Similar to the relations developed for solute dispersion, the particle dispersion coefficient is linearly dependent on the interstitial velocity:

$$D_{ij} = \alpha_L \overline{V} \delta_{ij} + (\alpha_L - \alpha_T) \frac{\overline{V_i}\,\overline{V_j}}{\overline{V}} + D_d T \delta_{ij} \tag{7}$$

where $\overline{V_i}$ is the component of the spatially distributed interstitial velocity along direction i, D_d is the colloid diffusion coefficient obtained from the Stokes-Einstein equation, α_L and α_T are the longitudinal and transverse dispersivities, respectively, and T is the porous medium tortuosity.

To appropriately describe the dynamic aspects of colloid deposition or release, the mass transport equation should be expressed in terms of colloid number concentration rather than mass concentration [Johnson and Elimelech, 1995; Johnson et al., 1996], that is

$$\frac{\partial n}{\partial t} = \nabla \cdot (D \cdot \nabla n) - \nabla \cdot (Vn) - \frac{f}{\pi \alpha_p} \frac{\partial \theta}{\partial t} \tag{8}$$

where n is the number concentration of colloids, θ is the fractional surface coverage, defined as the total cross section area of deposited colloids per interstitial surface area of the porous medium solid matrix, f is the specific surface area (i.e., interstitial surface area per porous medium pore volume), and α_p is the radius of colloidal particles. It can be readily shown that Eqn. 8 is equivalent to Eqn. 6.

Colloid Deposition and Release. Using the patchwise model for geochemical heterogeneity, the particle surface coverage rate of mineral grains is given by [Johnson et al., 1996]

$$\frac{\partial \theta}{\partial t} = \lambda \frac{\partial \theta_f}{\partial t} + (1-\lambda) \frac{\partial \theta_u}{\partial t} \tag{9}$$

When considering the dynamic aspects of particle deposition and release, the rate equations corresponding to the favorable and unfavorable surface fractions can be expressed as

$$\frac{\partial \theta_f}{\theta t} = \pi \alpha_p^2 k_{dep,f}\, n B(\theta_f) - k_{\det,f} \theta_f R(\theta_f) \tag{10a}$$

$$\frac{\partial \theta_u}{\theta t} = \pi \alpha_p^2 k_{dep,f}\, n B(\theta_u) - k_{\det,u} \theta_u R(\theta_u) \tag{10b}$$

where the subscripts f and u represent the favorable (λ) and unfavorable (1-λ) REV surface fractions, respectively, k_{dep} is the colloid deposition rate coefficient, k_{det} is the first order colloid release rate coefficient, and $B(\theta)$ and $R(\theta)$ are the dynamic blocking and release functions, respectively. The colloid deposition rate coefficient is related to the single collector efficiency η commonly used in filtration theories as [Elimelech et al., 1995]

$$k_{dep} = \frac{\eta V}{4\varepsilon} = \frac{\alpha \eta_0 V}{4\varepsilon} \tag{11}$$

where V is colloid advection velocity, ε is the porosity of the porous medium, α is the collision efficiency, and η_0 is the favorable single collector removal efficiency.

The dynamic blocking function $B(\theta)$ describes the probability of a colloid contacting a portion of collector surface unoccupied by previously deposited colloids [Song et al., 1994]. It accounts for the blocking effect of deposited colloids on the particle deposition rate. Two types of dynamic blocking functions are generally recognized: Langmuirian dynamic blocking function and random sequential adsorption (RSA) dynamic blocking function. Recent experimental investigations have shown that the RSA model describes the dynamics of particle deposition in porous media much better than the conventional Langmuirian model [Johnson and Elimelech, 1995; Johnson et al., 1996].

The general form of the RSA dynamic blocking function is [Adamczyk et al., 1992]

$$B(\theta) = 1 - a_1\left(\frac{\theta}{\theta_{max}}\right) + a_2\left(\frac{\theta}{\theta_{max}}\right)^2 + a_3\left(\frac{\theta}{\theta_{max}}\right)^3 \tag{12}$$

where θ_{max} is the maximum attainable surface coverage, a_1 and a_2, a_3 are coefficients that can be found theoretically (for ideal particles and collector surfaces) or empirically. The coefficients used by Johnson and Elimelech [1995] for $B(\theta)$ will be used in this colloid transport model as they were found adequate to describe the dynamics of blocking in flow of monodisperse latex microspheres in columns packed with spherical and uniform glass beads [Johnson and Elimelech, 1995]. Because colloid deposition onto the favorable surface fraction is usually irreversible, the RSA model can be used to describe the dynamics of particle deposition onto the favorable surface fraction. A similar dynamic blocking function was also chosen to describe the blocking of the unfavorable fraction, although the deposition onto the unfavorable surface fraction was assumed to be reversible with a non-zero release rate. This assumption, however, has negligible effect on the colloid transport behavior since the deposition rate on the unfavorable surface fraction is much smaller than on the favorable fraction, and the maximum surface coverage for the unfavorable surface fraction is much smaller than the maximum surface coverage on the favorable surface fraction.

Somewhat analogous to the dynamic blocking function, the dynamic release function describes the probability of colloid

release from porous media surfaces covered by retained colloids. In principle, this function should depend on the colloid residence time and the retained colloid concentration [Johnson et al., 1996]. When $R(\theta) = 1$, the release terms in Eqn. 10 represent first order kinetics release mechanism. Because at the present time the mechanisms of colloid release are poorly understood, only a first order release rate will be used in this paper.

Correlation between Physical Heterogeneity and Colloid Deposition Rate. In modeling colloid transport, the variation of flow field will change the colloid concentration distribution in the studied domain not only by affecting hydrodynamic dispersion and advection, but also by influencing the colloid deposition rate. For Brownian colloids where deposition rate is controlled by a convective-diffusive mechanism [Elimelech et al., 1995] there exists a positive relationship between the hydraulic conductivity and the particle deposition rate. Based on Eqn. 11, the colloid deposition rate (k_{dep}) is proportional to ($\eta_0 V$), with η_0 for Brownian colloids being proportional to $V^{-2/3}$ [Elimelech et al., 1995]. Hence, combining this relationship with Darcy's law one obtains that the colloid deposition rate (k_{dep}) is proportional to $K^{1/3}$. A consequence of this relationship is that a random field of hydraulic conductivity leads to a random field of colloid deposition rate as well.

We assume that $P(x) = \ln k_{dep}(x)$ is normally distributed with a mean <P> and variance σ_P^2, and has a similar form of the covariance function as the hydraulic conductivity field. To describe the correlation between the random hydraulic conductivity field and the colloid deposition rate, it is further assumed that

$$P = \langle P \rangle + \omega P' + \gamma Y' \tag{13}$$

where ω and γ are correlation coefficients and Y' is the perturbation of the hydraulic conductivity field. When $\omega = 0$ and $\gamma > 0$, P and Y are perfectly positively correlated; when $\omega = 0$ and $\gamma < 0$, P and Y are perfectly negatively correlated; and when $\omega \neq 0$, P and Y are not perfectly correlated. For Brownian colloids, $\omega = 0$ and $\gamma > 0$; the value of γ is chosen as 1/3, for the reason discussed above.

Numerical Procedures. In the colloid transport model presented in the previous section, the transient flow equation is coupled to the colloid transport equation. Numerical solution can be obtained with both transient and steady state flow fields using the multiple cell balance (MCB) method [Sun, 1995]. The flow region in our model is a vertical rectangular domain, with the horizontal x axis ranging from 0 to 3 m and the vertical z axis ranging from 0 and 1 m. The computational domain Ω is encircled by the line boundary Γ.

Initial and Boundary Conditions. For the flow equation, the initial and boundary conditions for the flow domain are specified as follows:

$$h(x) = h_0 \quad \text{at} \quad t = 0 \tag{14a}$$

$$h(0,z,t) = h_1 \quad \text{for} \quad t > 0,\ (0,z) \in \Gamma_1 \tag{14b}$$

$$\left.\frac{\partial h(x,z,t)}{\partial z}\right|_{z=0} = 0 \quad \text{for} \quad t > 0,\ (x,0) \in \Gamma_2 \tag{14c}$$

$$\left.\frac{\partial h(x,z,t)}{\partial z}\right|_{z=1} = 0 \quad \text{for} \quad t > 0,\ (x,1) \in \Gamma_3 \tag{14d}$$

$$h(3,z,t) = h_2 \quad \text{for} \quad t > 0,\ (3,z) \in \Gamma_4 \tag{14e}$$

where $\Gamma = \Gamma_1 \cup \Gamma_2 \cup \Gamma_3 \cup \Gamma_4$, and h_1 and h_2 are fixed values of hydraulic heads on the boundaries.

The initial and boundary conditions for the colloid transport equation are specified as follows. Initially the porous medium has no deposited colloids (i.e., zero surface coverage, $\theta_f = \theta_u = 0$). At the four boundaries (Γ), zero dispersive flux boundary conditions are specified. Furthermore, a given concentration of colloids is injected into the domain at $t>0$. The type of colloid injection can be classified as pulse injection or continuous injection depending on the duration of the injection. The mode of injection can be characterized as point injection or line injection based on the number and locations of injection wells. The injection is set as the boundary condition for the colloid concentration.

Multiple Cell Balance Algorithm. Because there are no analytical solutions for the flow and colloid transport governing equations, we adopted the multiple cell balance (MCB) method [Sun and Yeh, 1983] to solve the two-dimensional transport model numerically. The MCB method was originally derived for solving the coupled groundwater flow and solute transport equations for solutes experiencing equilibrium sorption [Sun, 1995]. The method has never been applied to the more complex problem of colloid transport. The details on the numerical formulation and procedures are given in the doctoral dissertation of Sun [Sun, 1998].

Validation of the Numerical Code. Previous studies suggested the MCB method provides adequate solution for two-dimensional non-reacting solute transport problems [Sun, 1995]. We compared the numerical solution based on our MCB code for the transport of a tracer in a two-dimensional semi-infinite isotropic porous medium with the analytical solution provided by Leij and Dane [1990]. The numerical results closely agreed with the analytical solution. To validate the MCB code for colloid transport, the analytical solution derived by Lapidus and Amundson [1952] for the one-dimensional solute transport problem with finite rates of sorption (k_1) and desorption (k_2) was compared with our numerical solution for the following problem:

$$\frac{\partial C}{\partial t} = D_L \frac{\partial^2 C}{\partial x^2} - V\frac{\partial C}{\partial t} - \frac{\rho_b}{\varepsilon}\frac{\partial S}{\partial t} \tag{15}$$

$$\frac{\partial S}{\partial t} = k_1 C - k_2 S \tag{16}$$

The initial concentration is set at zero, the concentration at the inlet boundary is given as a constant C_0, and the dispersive flux of colloid is set at zero to the outlet boundary. The analytical solution of Lapidus and Amundson [1952] is given by

$$\frac{C}{C_0} = e^{\frac{Vx}{2D}}\left[F(t) + k_2 \int_0^t F(\tau)d\tau\right] \tag{17}$$

where

$$F(t) = e^{-k_2 t}\int_0^t I_0\left[2\sqrt{\frac{k_1 k_2 \rho_b \tau}{\varepsilon}(t-\tau)}\right]\frac{x}{2\sqrt{\pi D \tau}}\, e^{\frac{x}{4Dr} - \tau d}\, d\tau \tag{18}$$

and

$$d = \frac{V^2}{4D} + \frac{k_1 \rho_b}{\varepsilon} - k_2 \qquad (19)$$

As shown in Figure 7, the numerical results obtained from the MCB code are in very close agreement with the analytical solution.

Results and Discussion

The newly developed 2-D colloidal transport model is used to conduct a numerical investigation of colloidal transport in physically and geochemically heterogeneous porous media. We first illustrate the effect of key model parameters on the general colloid transport behavior. This follows by a systematic investigation of colloid transport in layered as well as randomly heterogeneous subsurface porous media.

Influence of Key Model Parameters. The basic values of the model parameters and the range of their variation during the numerical investigation are listed in Table 17. The range of parameter values covers possible scenarios of colloid transport in sandy aquifers, such as the glacial outwash sandy aquifer in Cape Cod, Massachusetts, which has been used extensively in field investigations [LeBlanc et al., 1991; Garabedian et al., 1991; Hess et al., 1992; Gelhar et al., 1992; Sun, 1995; Harvey et al., 1989; Ryan and Gschwend, 1990; McCarthy and Degueldre, 1993; Johnson et al., 1996; Pieper et al., 1997]. Colloidal particles are introduced at the boundary $x = 0$ as a pulse injection with a duration of 0.5 days. The results (Figure 8) are presented as relative colloid concentration n/n_0 along the flow direction x at a certain observation time ($t = 0.75$ d).

Under the examined conditions, an increase in hydraulic conductivity results in enhanced colloid migration and a wider spreading of the colloid concentration profiles (Figure 8a). With a constant hydraulic head gradient, a greater hydraulic conductivity results in larger flow velocity so that the colloid advection velocity increases. Because the particle dispersion coefficient is proportional to the colloid advection velocity, dispersion (spreading) of colloids also increases as the hydraulic conductivity is increased. In addition, the capture of colloids traveling through the porous medium decreases with increasing flow velocity, thus resulting in a slightly attenuated particle concentration profile.

Hydrodynamic dispersion is also controlled by the longitudinal and transverse dispersivities (Eqn. 7). The ratio of longitudinal dispersivity to transverse dispersivity is typically in the range of 5 to 20 [Sun, 1995]. We assumed a ratio of 5 and investigated the effect of varying the longitudinal dispersivity. Because longitudinal dispersivity is scale dependent, and our problem is of local scale (*ca.* 3 m), only a narrow range of values was selected for the longitudinal dispersivity. The results (Figure 8b) show that small changes in longitudinal dispersivity lead to relatively large changes in the colloid concentration profiles.

To investigate the effect of particle deposition rate, a constant geochemical heterogeneity (λ=0.01) was assumed. We fixed the favorable particle deposition rate coefficient, and adjusted the unfavorable deposition rate by choosing different values for the collision efficiency of the unfavorable surface fraction α_u. The results (Figure 8c) show that particle deposition rate can substantially affect the colloid concentration profile. As the collision efficiency α_u increases, the colloid deposition rate on the unfavorable fraction increases, and less colloids can be detected in the aqueous phase. The magnitude of the collision efficiency α_u reflects the effect of changes in the solution chemical composition.

By fixing the particle deposition rate coefficients $k_{dep,f}$ and $k_{dep,u}$, the overall particle deposition rate can be controlled by the geochemical heterogeneity parameter λ. The marked effect of geochemical heterogeneity on colloidal transport is illustrated in Figure 8d. An increase in geochemical heterogeneity results in increased overall colloid deposition rate and reduced concentration of colloids in bulk solution. For the conditions investigated in Figure 8d, a substantial geochemical heterogeneity of subsurface porous media (>10%) may result in nearly complete immobilization

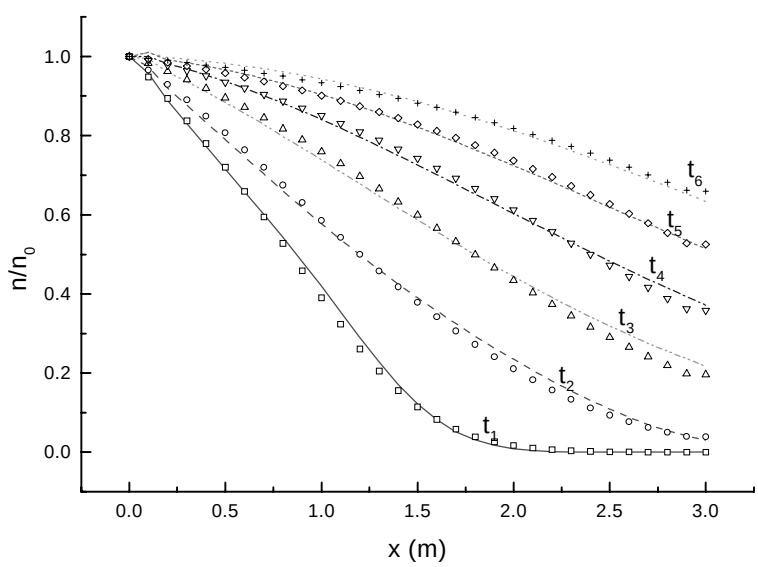

Figure 7. Comparison of numerical solutions (symbols) with analytical solutions (lines) for reactive solute transport in isotropic semi-infinite porous medium. The parameters used for this simulation are V_{Darcy} = 1.0 m s^{-1}; α_L = 0.05 m, α_L: α_T = 5:1; Pe_L = 1; Courant No. = 0.25-1.0. The observation times from t_1 to t_6 are 0.5, 1.0, 2.0, 3.0, 4.0, 5.0 d.

Table 17. Basic values and ranges for parameters in the colloid transport model.

parameter	value	range
hydrologic parameters		
∇h	10^{-2}	10^{-4}~10^{-1}
$\boldsymbol{K}$ (m d^{-1})	10^{2}	10^{0}~10^{3} m/day
S_S	10^{-4}	
α_L (m)	0.05	0.01~0.7 m
α_L/α_T	5	5~20
ε	0.4	0.3~0.5
transport parameters		
d_c (mm)	0.3	
f [a] (m^2/m^3)	30000	
d_p (μm)	0.3	0.01~1
ρ_p (g cm^{-3})	2.5	
C_0 (mg L^{-1})	10	
n_0 (# m^{-3})	2.8×10^{14}	10^{11}~10^{15}
α	10^{-3}	10^{-4}~10^{0}
η_0 [b]	0.0259	
λ (%)	0.1	0.1~10
$k_{dep,u}$ [c] (m d^{-1})	6.5×10^{-6}	
$k_{dep,f}$ [c] (m d^{-1})	6.5×10^{-3}	
$k_{det,u}$ (hr^{-1})	0.0	10^{-4}~10^{-2}
$k_{det,f}$	0.0	0.0

[a] *Determined from $3(1-\varepsilon)/(\varepsilon a_c)$*
[b] *Determined from the method of Elimelech and Song [1992].*
[c] *Determined from Eqn. 11.*

of colloidal particles as shown by the flat, attenuated colloid concentration profile.

The colloidal transport model assumes that particle deposition onto the favorable surface fraction is irreversible; hence, the colloid release rate from the favorable surface fraction is zero. This assumption has been confirmed in particle deposition studies involving oppositely charged particles and collector surfaces [Elimelech et al., 1995]. On the other hand, in particle deposition studies involving similarly charged particles and collector surfaces, a finite rate of colloid release can be detected [Ryan and Elimelech, 1996]. Hence, we investigated the effect of colloid release rate from the unfavorable surface fraction on the colloid concentration profile as shown in Figure 8e. The results demonstrate that larger release rate coefficients result in increased colloid concentration in the aqueous phase, whereas smaller release rate coefficients have no effect on the colloid concentration profile. Since the colloid release rate depends on the concentration of deposited particles (first order kinetics), the effect of colloid release on the colloid concentration profile depends on the overall colloid deposition rate onto the unfavorable surface fraction. Figure 8f demonstrates that the model solution is very sensitive to particle size. Particle size influences colloidal transport mainly through its effect on colloid deposition rate. As expected for deposition of Brownian particles, which is controlled by a convective-diffusion mechanism, the deposition rate becomes smaller as particle size increases. Consequently, larger particles migrate faster in the porous medium and their concentration in the liquid phase is greater than that of smaller particles.

Colloid Transport in Layered Heterogeneous Porous Media. The porous medium was divided into three horizontal layers, parallel to the flow direction. The layers are denoted as layer I (0-0.3 m), layer II (0.3-0.7 m), and layer III (0.7-1.0 m) from bottom to top. Layers I and III were assigned the same heterogeneity parameter values, whereas a different parameter value was assigned to the middle layer II. The colloid suspension was assumed to be fed continuously (line injection) into the porous

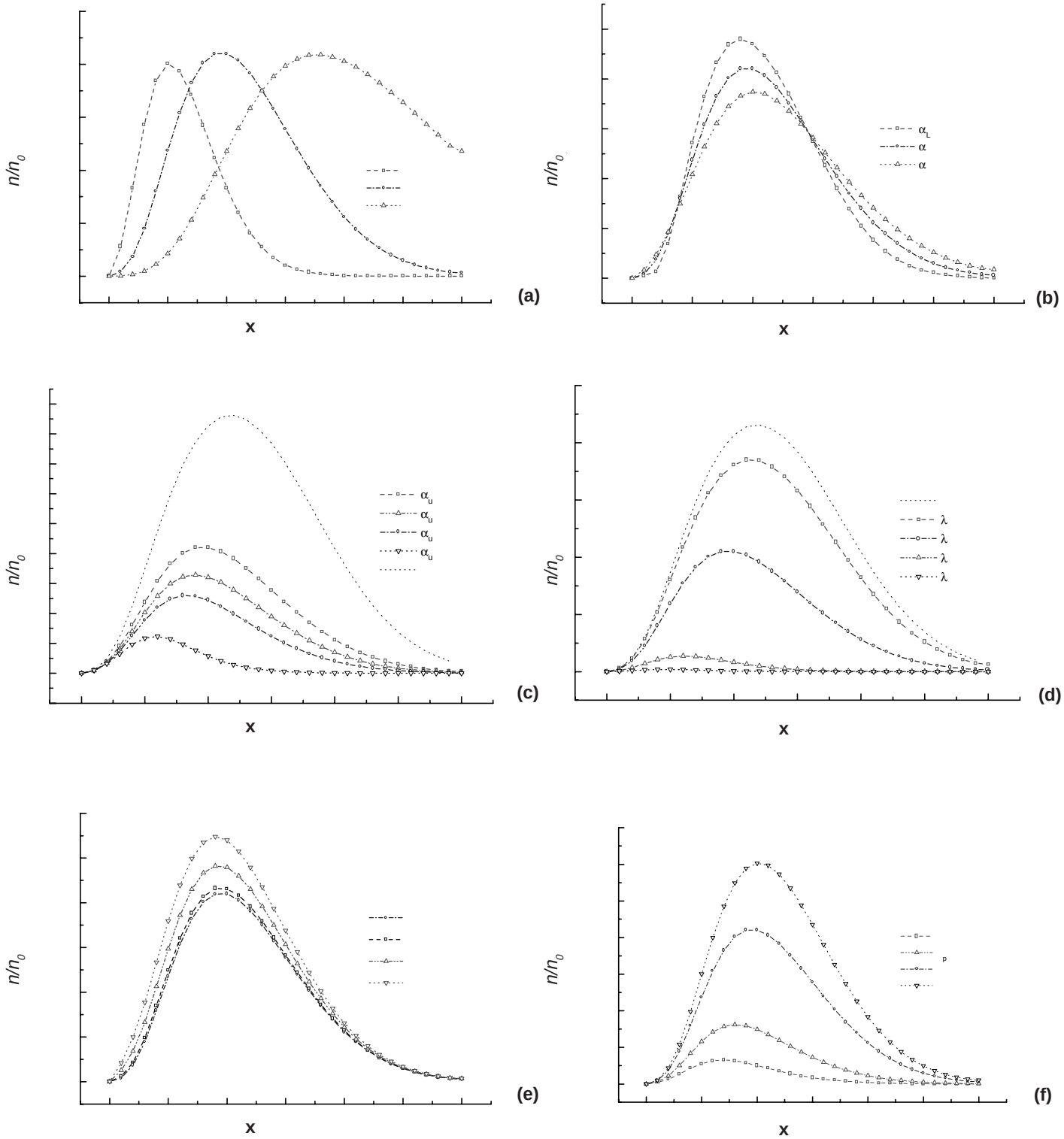

Figure 8. The role of model parameters in colloid transport in physically homogeneous porous media. The results are presented as relative colloid concentration n/n_0 along the flow direction x at a certain observation time (t = 0.75 d). The effects of (**a**) hydraulic conductivity, (**b**) longitudinal dispersivity, (**c**) collision efficiency (deposition rates), (**d**) geochemical heterogeneity, (**e**) release rate from unfavorable surface fraction; and (**f**) particle size on colloid concentration profile along z = 0.5 m. Parameter values are shown in Table 17.

medium at the inlet boundary (x=0), with 11 injection points set at 0.1 m intervals along the z direction. Observations of concentration profiles over the entire two-dimensional porous medium domain are presented for t=0.75 d. The physical and geochemical heterogeneity parameter values used in the numerical investigation (represented by K and λ, respectively) were comparable to those reported for the Cape Cod sandy aquifer [Leblanc et al., 1991].

The effect of layer-distributed physical heterogeneity on colloid transport is illustrated in Figure 9. The hydraulic conductivity of the middle layer (layer II) of the porous medium is twice as large as the hydraulic conductivity in the layers above and below. Therefore, the fluid flows in the central layer faster than the other two layers, and most of the colloids migrate with the flow through the more permeable layer. This example points out the paramount importance of preferential flow paths in colloid transport.

Because transverse dispersion reduces the amount of colloids passing through the preferential flow path, the role of longitudinal and transverse dispersivities was also investigated. Two different ratios of longitudinal to the transverse dispersivities (1 and 10) were studied, as shown in Figure 10. When the transverse dispersion is relatively large (α_L/α_T=1.0), the extent of preferential flow in the middle (most permeable) layer of the porous medium is reduced (Figure 11a). However, when the transverse dispersion is relatively small (α_L/α_T=10.0), the preferential transport of colloids in the middle layer of the porous medium is enhanced (Figure 11b). The results demonstrate that hydrodynamic dispersion can influence colloid transport in layered heterogeneous porous media, but the effect is not strong enough to explain the preferential transport of colloidal particles.

The effect of a layered geochemical heterogeneity on colloid transport in physically homogeneous (constant hydraulic conductivity) subsurface porous medium is shown in Figure 12. The central layer had a very small value of geochemical heterogeneity (λ=0.001), whereas the upper and lower layers had much higher values (λ=0.025). The results clearly show that the increased particle deposition rate of colloids onto the favorable surface fractions of the more heterogeneous (lower and upper) layers can result in preferential flow of colloidal particles through the middle layer, similar to that observed for layered, physically heterogeneous porous media.

Because subsurface porous media are physically as well as geochemically heterogeneous, it is of great interest to investigate the combined effect of layered physical and geochemical heterogeneity. For the layered physically heterogeneous porous medium shown in Figure 9, we assumed that the geochemical heterogeneity is layered distributed as well. Figure 11a illustrates the results when the central layer has a larger λ(0.025) compared to the two side layers (λ=0.001). It is interesting to note that for these conditions the preferential flow path (initially caused by the physical heterogeneity, Figure 9) disappears due to the geochemical heterogeneity. On the other hand, the preferential flow path is enhanced when the middle layer has a smaller λ(0.001) than the two side layers (λ=0.025), as shown in Figure 11b. The results clearly demonstrate that layered geochemical heterogeneity can significantly alter the preferential transport of colloidal particles caused by heterogeneous flow field. Hence, consideration of physical or geochemical heterogeneity alone in colloidal transport models may result in erroneous results.

Colloid Transport in Randomly Heterogeneous Porous Media. Colloid transport in randomly heterogeneous porous media is investigated in this section. The numerical investigation is carried out for a point injection (at x=0.5m, z=0.5m) with a pulse duration of 0.1 day. Results are presented as snapshots of colloid concentration in the porous medium at t=0.5 day.

Freeze [1975] pointed out that hydraulic conductivity variations in aquifers are typically lognormally distributed with a standard deviation (in log base 10 units) ranging from 0.2 to 2.0. Since then, several field measurements confirmed this observation. For instance, it was reported that the mean hydraulic conductivity K for the Borden site is 0.0072 cm/s with the variance of ln$K$ being 0.29 [Sudicky, 1986]. Hufschmied [1986] reported that the mean value of K is 0.36 cm/s for the Aefligen site with a

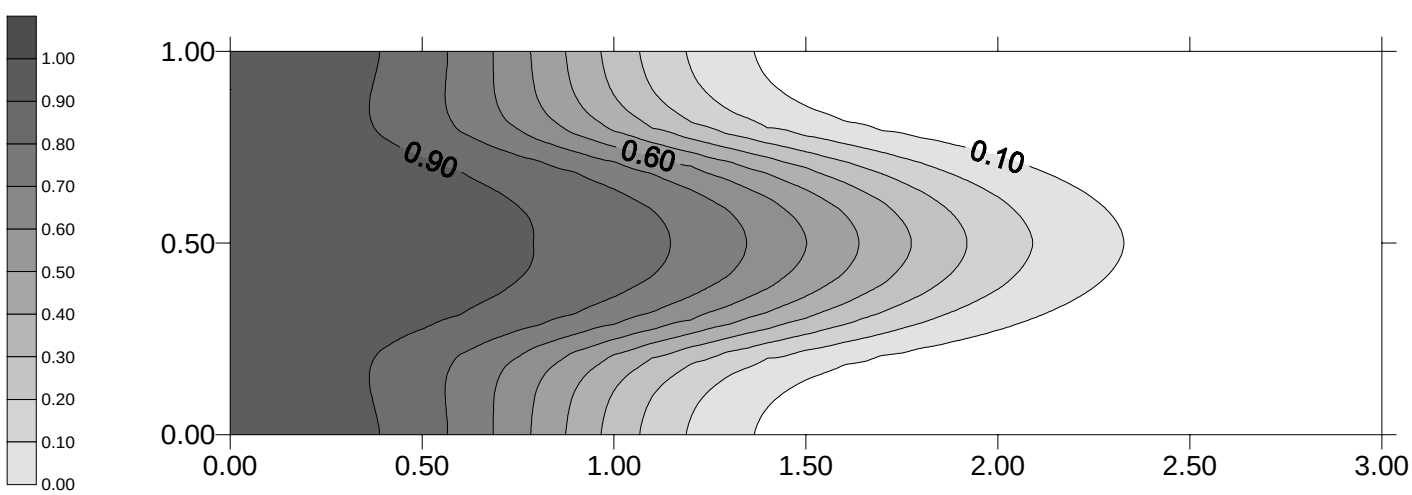

Figure 9. Effect of layered physical heterogeneity of porous media on colloid transport. The hydraulic conductivity of the central layer is K=100m d^{-1}. The hydraulic conductivities of the upper and lower layers are K = 50 m d^{-1}. The geochemical heterogeneity for all the layers is the same, λ=0.01; α_L/α_T=5. The x and z axes show distance (m). The bar graph shows the colloid concentration in the porous medium normalized to the influent colloid concentration at x = 0.

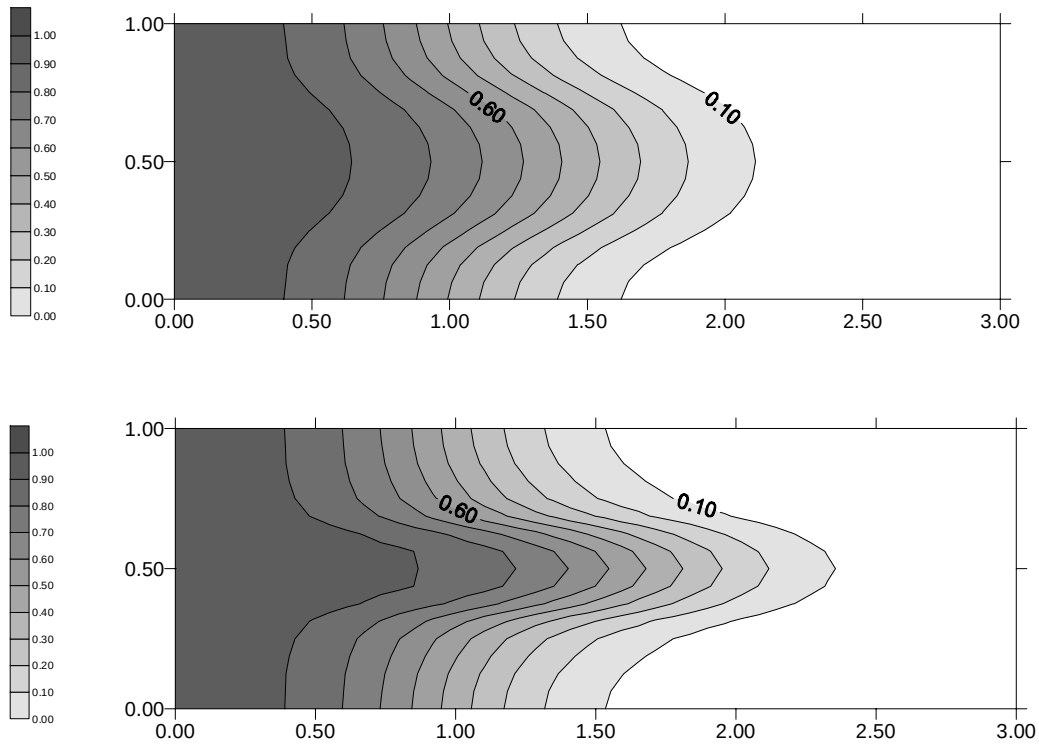

Figure 10. Effect of the ratio of a_L to a_T on the preferential flow of colloids caused by layered physical heterogeneity of porous media: (**a**) $\alpha_L/\alpha_T = 1$; (**b**) $\alpha_L/\alpha_T = 10$. The *x* and *y* axes show distance (m). The bar graph shows the colloid concentration in the porous medium normalized to the influent colloid concentration at $x = 0$.

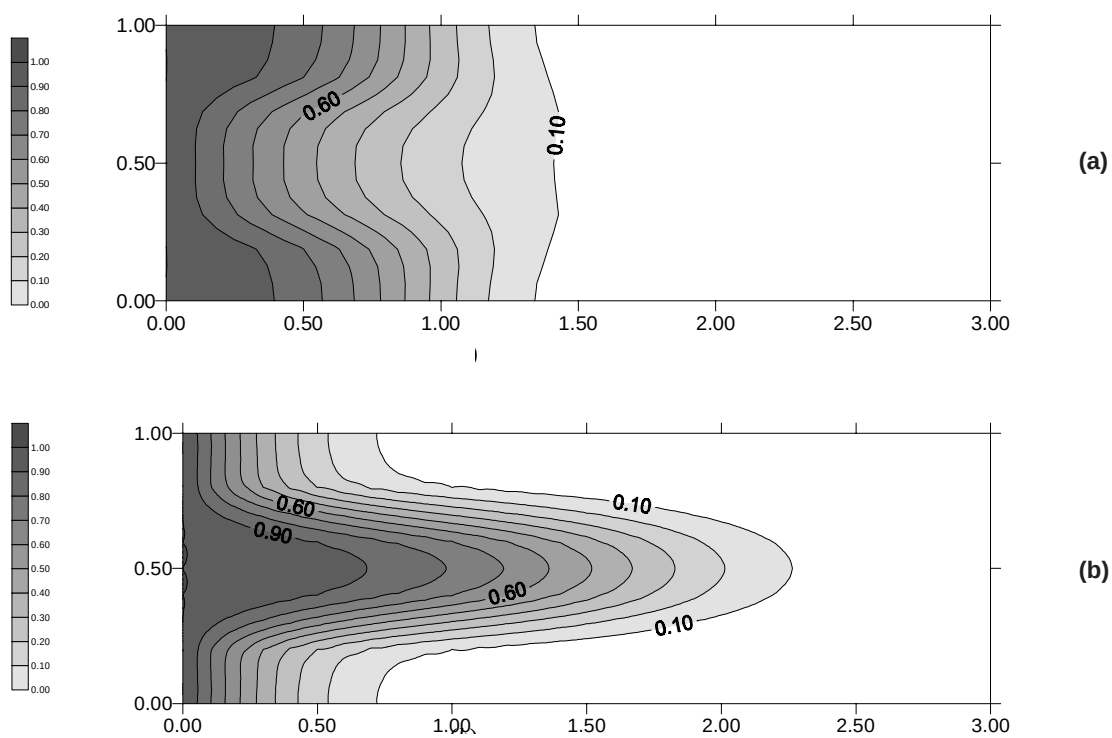

Figure 11. Effect of layered geochemical and physical heterogeneity of porous media on the preferential flow of colloids: (**a**) central layer, $K = 100$ m d^{-1}, $\lambda = 0.025$; upper and lower layers contain $K = 50$ m d^{-1}, $\lambda = 0.001$; $\alpha_L/\alpha_T = 5$; (**b**) central layer, $K = 100$ m d^{-1}, $\lambda = 0.001$; upper and lower layers contain $K = 50$ m d^{-1}, $\lambda = 0.025$; $\alpha_L/\alpha_T = 5$. The *x* and *y* axes show distance (m). The bar graph shows the colloid concentration in the porous medium normalized to the influent colloid concentration at $x = 0$.

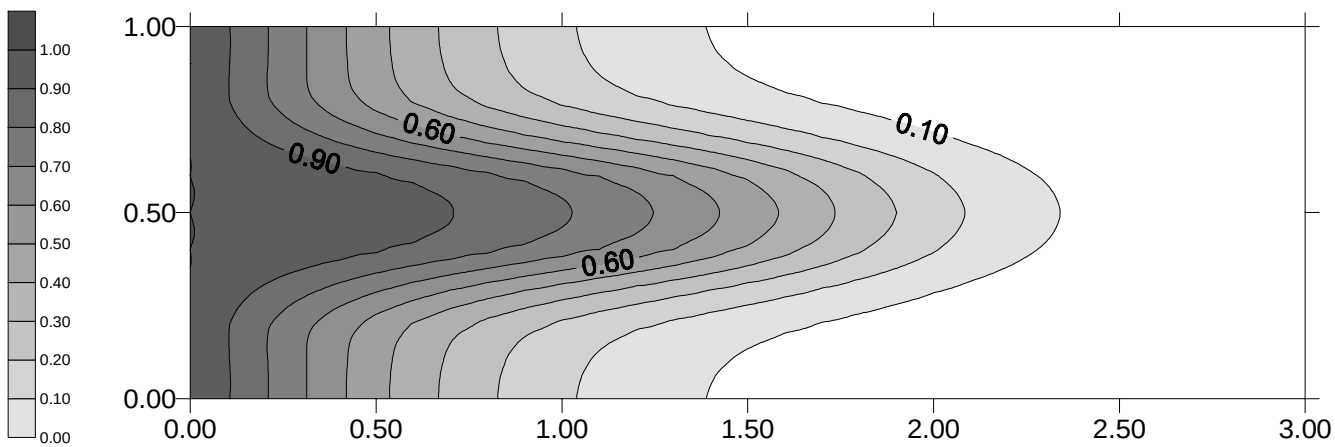

Figure 12. The preferential flow of colloids caused by the layered geochemical heterogeneity in a physically homogeneous porous medium. The geochemical heterogeneity of the central layer is λ=0.001; the geochemical heterogeneity of the upper and lower layers is λ=0.025. Hydraulic conductivity K = 100 m d^{-1} for each layer; α_L/α_T=5. The x and z axes show distance (m). The bar graph shows the colloid concentration in the porous medium normalized to the influent colloid concentration at x = 0.

variance of ln$K$ of 2.15. The horizontal (x, y directions) and vertical (z direction) correlation scales were reported to be 0.29, 2.8, and 0.12 m, respectively, for the Borden site [Sudicky, 1986]; 0.26, 5.1, and 0.26 m, respectively, for the Cape Cod site [Hess, 1989]; and 0.031, 3.0, and 0.91 m, respectively, for the Twin Lakes site [Moltyaner, 1986].

In our study, the mean value of K was set at 0.116 cm s^{-1} (100 m d^{-1}), the variance of ln$K$ was set at 0.24 or 2.4, and the correlation scale of the vertical porous medium was set as 0.5 m. The random field of hydraulic conductivity was generated numerically as outlined earlier in this paper, and was incorporated into the MCB code of colloid transport. Similar variance values were used to generate the random field of the particle deposition rates. The mean values of the deposition rate coefficients were set at 6.5x10^{-3} m d^{-1} for the favorable surface fraction and at 6.5x10^{-6} m d^{-1} for the unfavorable surface fraction. Note that the latter corresponds to α_u=10^{-3}.

Realizations of the random fields of hydraulic conductivity with two different variance values of ln$K$ (0.24 and 2.4) are shown in Figure 13. Figure 14 presents the corresponding hydraulic head distributions and colloid concentration profiles in the randomly physically heterogeneous porous media; the results for physically homogeneous porous media are presented as well. Compared to the physically homogeneous case, random fields of ln$K$ result in obvious irregular hydraulic head distributions (Figures 14b,c). The irregularity of the hydraulic head distributions increases with the variance of ln$K$. A similar trend can be observed in the colloid concentration profiles. When the variance of ln$K$ is small, the colloid concentration profile (Figure 15b) is only slightly different than the homogeneous case. However, a very irregular shape of the concentration profile (Figure 15c) can be seen when the variance of ln$K$ is large. The results clearly demonstrate that a random physical heterogeneity of porous media results in a random behavior of colloid transport as well.

Because of lack of field measurements on random geochemical heterogeneity of subsurface porous media, we conducted a preliminary numerical investigation on the sensitivity of the colloid transport behavior to the parameters characterizing the geochemical heterogeneity. Results indicated that the mean value of the geochemical heterogeneity has to be large enough (λ=0.01) to show the effect of its spatial distribution on the colloid concentration profiles. When the mean value of λ is as small as 0.001, which may be a reasonable value for sandy aquifers with negligible iron oxyhydroxide coatings, the distribution of λ apparently does not affect the colloid transport behavior, even when λ is assumed to have a lognormal distribution with a rather large variance. Therefore, a mean value of λ= 0.01 was chosen to carry out the rest of the numerical investigation. This value is quite reasonable for the geochemical heterogeneity of subsurface geological formations [Heron et al., 1994; Kretzschmar et al., 1995; Coston et al., 1995]. It was also found that a lognormally distributed field of λ with a relatively small variance does not have an observable effect on the particle concentration profiles; therefore, a variance of lnλ as large as 2.0 was chosen.

Realizations of the random fields of λ are shown in Figure 16. For a normal distribution, the standard deviation was chosen as large as 0.005. Of the simulated λ values, about 2.5% are negative; these negative values were truncated from the distribution. Figure 16a shows that the value of λ is mostly distributed from 0.0 to 0.02. For a lognormal distribution, the variance of lnλ was set as large as 2.0. We truncated about 2 %t values which are larger than 1.0. The value of λ varies mainly between 0.001 to 0.2, and some values of λ even reach 1.0 (Figure 16b).

The colloid concentration profiles for the two different geochemical heterogeneity fields are compared with the case of a constant λ in Figure 17. The normally distributed random field of geochemical heterogeneity apparently does not affect the colloid concentration profiles (Figure 17b). A lognormal field of geochemical heterogeneity with a large variance (Figure 17c) developed only a slight irregularity in the concentration profile. These results suggest that the effect of a random field of

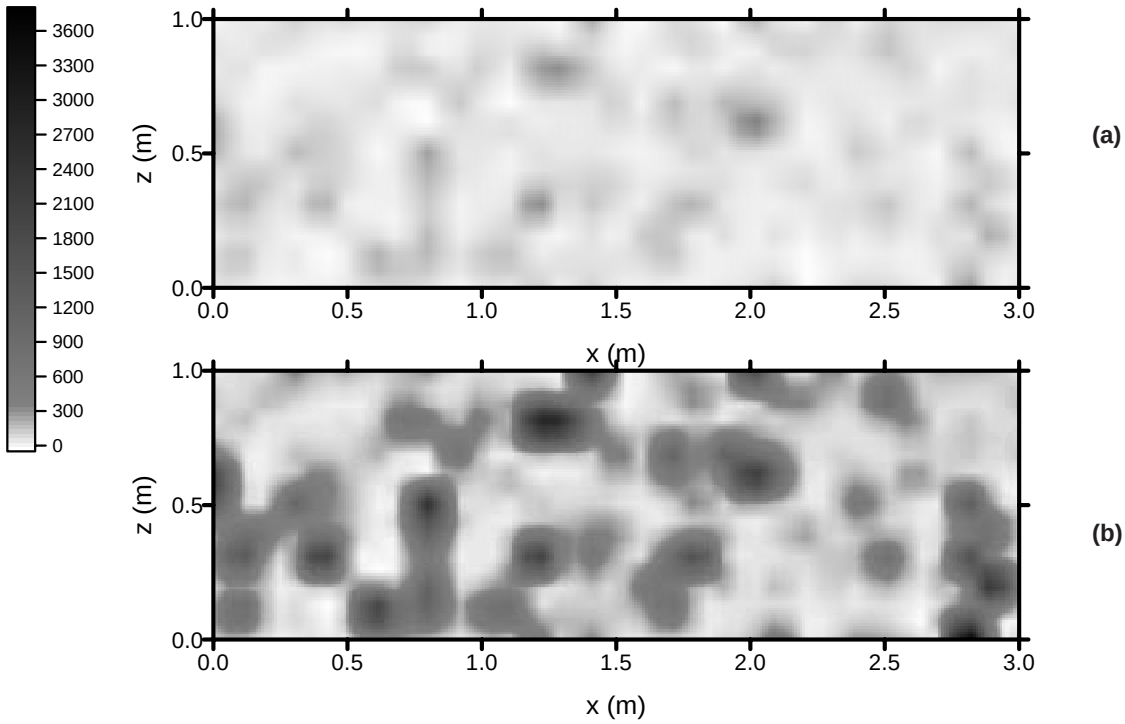

Figure 13. The realizations of random hydraulic conductivity fields. The scale bar on the left represents hydraulic conductivity (m d^{-1}): (**a**) E(K) = 100 m d^{-1}, Var(ln$K$) = 0.24; (**b**) E(K) = 100 m d^{-1}, Var(ln$K$) = 2.4. The x and z axes show distance (m).

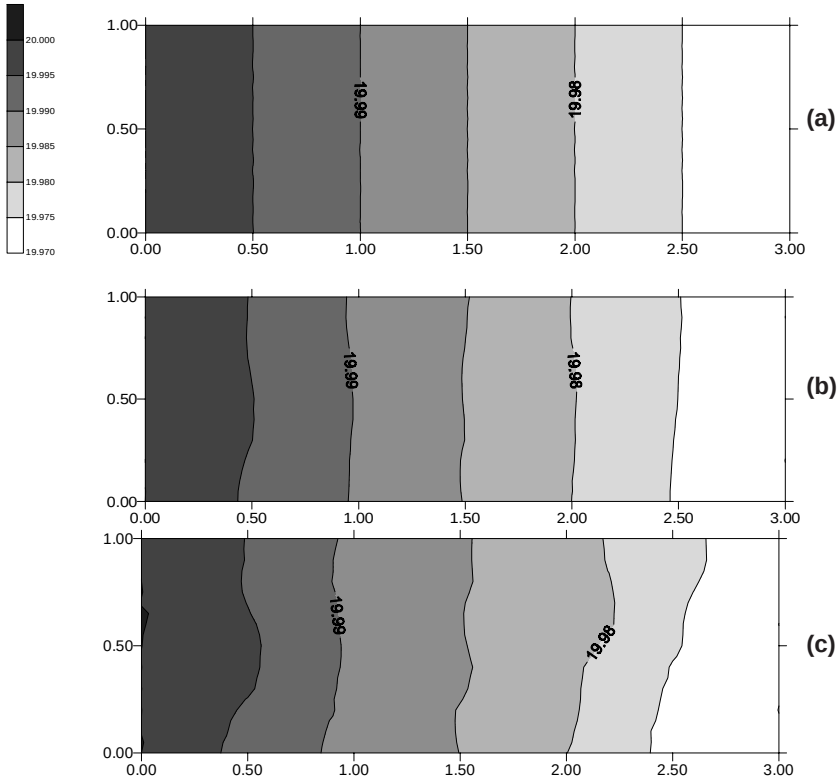

Figure 14. The hydraulic head distributions in homogeneous or randomly physically heterogeneous porous media. (**a**) E(K) = 100 m d^{-1}, Var(ln$K$) = 0.0; the porous medium is physically homogeneous; (**b**) E (K) = 100 m d^{-1}, Var(ln$K$) = 0.24; (**c**) E(K) = 100 m d^{-1}, Var(ln$K$) = 2.4. The x and z axes show distance (m).

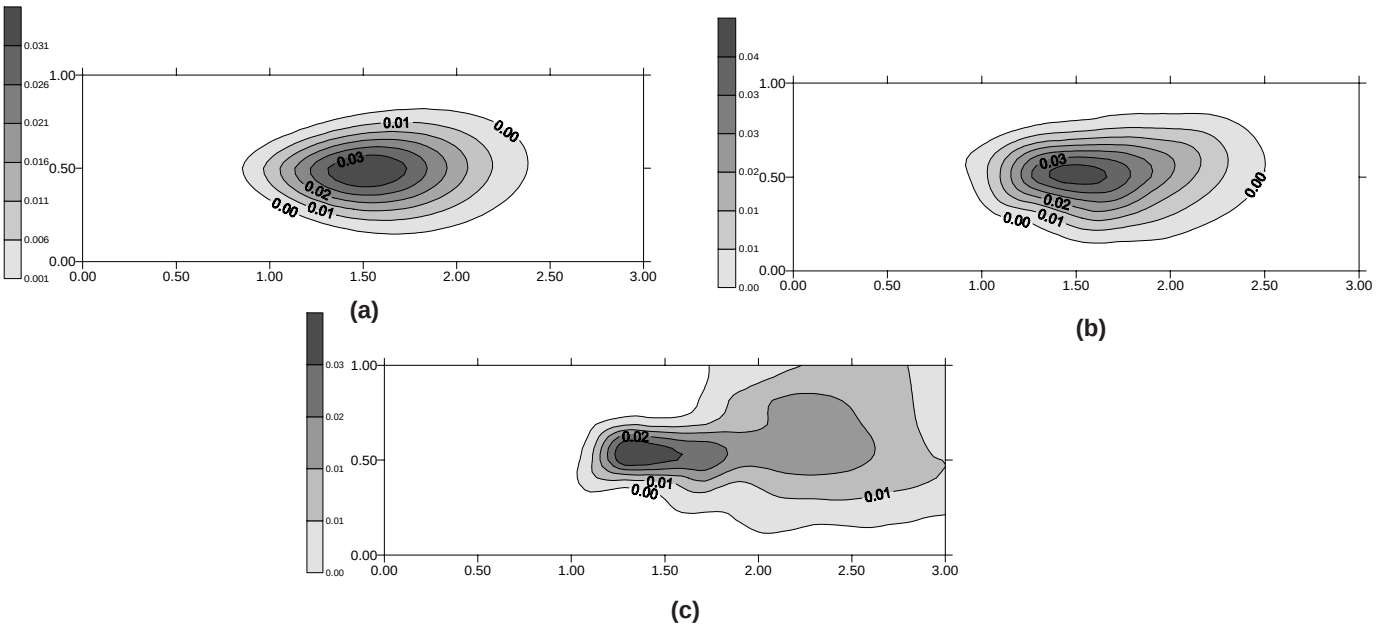

Figure 15. The colloid concentration profiles in a homogeneous or randomly physically heterogeneous porous medium for a point injection at (0.5 m, 0.5 m) with a duration of 0.1 d for a snapshot taken at 0.5 d: (**a**) E(K) = 100 m d^{-1}, Var(ln$K$) = 0.0; the porous medium is physically homogeneous; (**b**) E(K) = 100 m d^{-1}, Var(ln$K$) = 0.24; (c) E(K) = 100 m d^{-1}, Var(ln$K$) = 2.4. The x and z axes show distance (m).

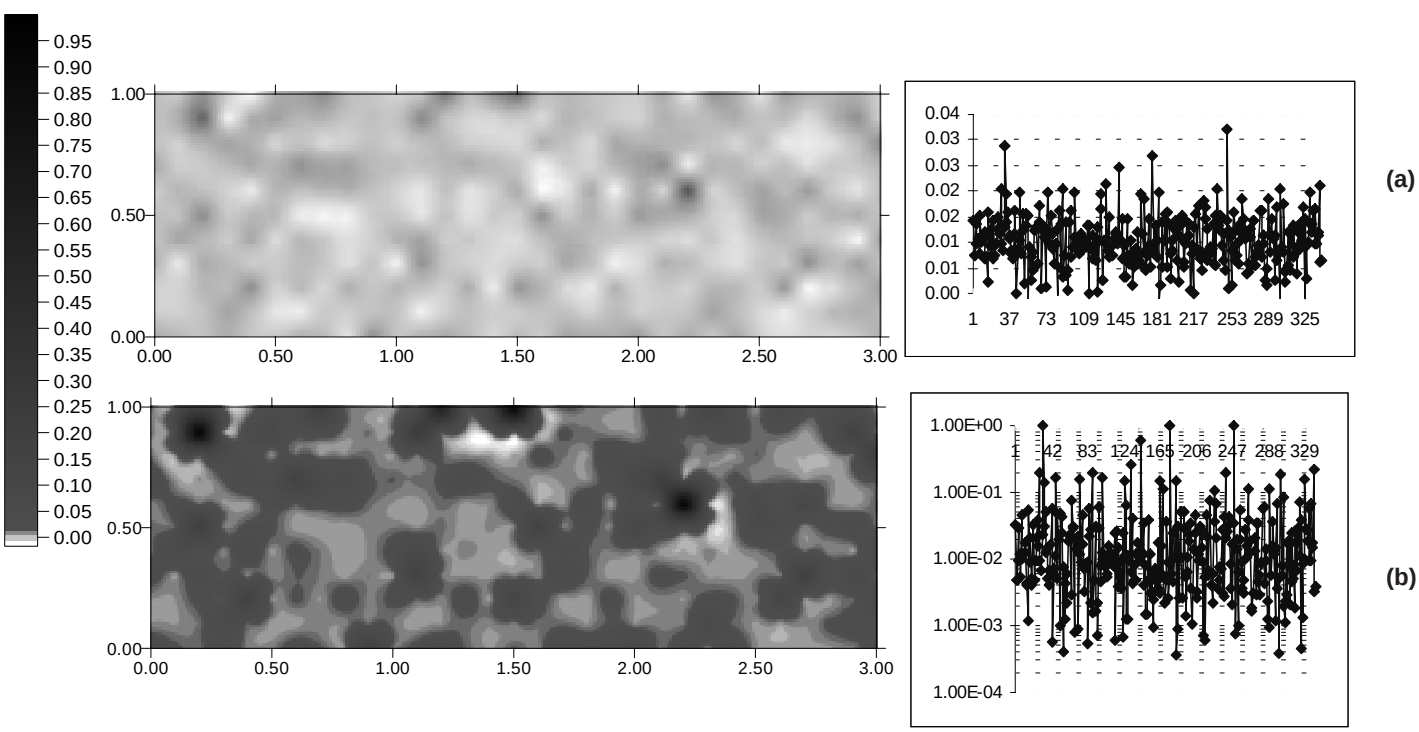

Figure 16. The realizations and value distributions of random geochemical heterogeneity fields. The gray bar values show the range of λ : (**a**) normal distribution with E(λ) = 0.01 and $\sigma(\lambda)$ = 0.005; (**b**) lognormal distribution with E(λ) = 0.01, and Var(lnλ) = 2.0. The x and z axes show distance (m).

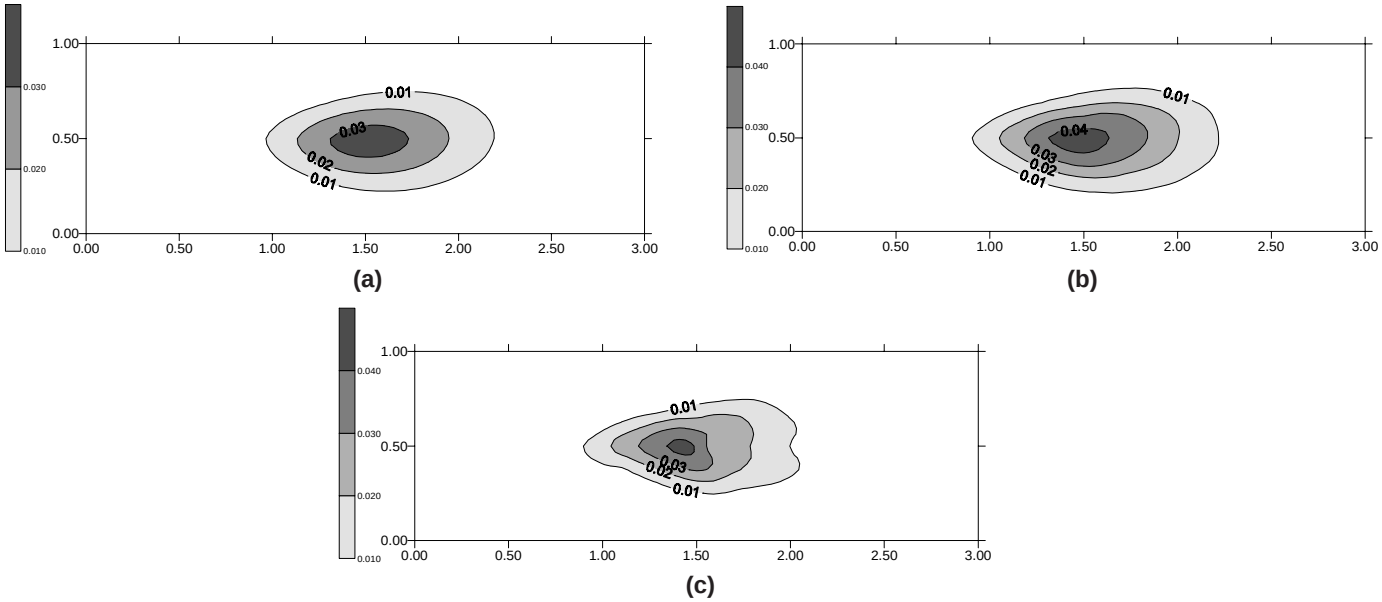

Figure 17. The effect of random geochemical heterogeneity on colloid transport for a snapshot at t = 0.5 d after a point release at (0.5 m, 0.5 m): (**a**) colloid concentration profile in a porous medium with a constant geochemical heterogeneity, λ=0.01; (**b**) colloid concentration profile in a normally distributed geochemically heterogeneous porous medium, E(λ) = 0.01, $\sigma(\lambda)$ = 0.005; (**c**) colloid concentration profile in a lognormally distributed geochemically heterogeneous porous medium.

geochemical heterogeneity on colloid transport is not as strong as the effect of random physical heterogeneity. Hence, the mean value of geochemical heterogeneity is more important than its distribution in modeling colloid transport in heterogeneous porous media.

Summary and Conclusions

The major objectives of this research were to (1) examine the dependence of colloid transport and mobilization on chemical perturbations, (2) assess the relative transport of mobilized colloids and the chemicals that caused their mobilization, and (3) develop a colloid transport model that would begin to describe these effects. Through the field tests, laboratory experiments, and model development designed to meet these objectives, we made significant advances toward testing the major hypothesis driving this research, that the transport of colloids mobilized in a contaminant plume will be limited by the advance of the chemical agent causing colloid mobilization.

The field tests were conducted in the uncontaminated and secondary sewage-contaminated zones of the ferric oxyhydroxide-coated quartz sand aquifer at the U.S. Geological Survey Toxic Hydrology Research Site on Cape Cod, Massachusetts. These experiments examined the dependence of colloid transport and mobilization on chemical perturbations and assessed the relative transport of mobilized colloids and the chemicals that caused their mobilization. The transport of mineral (silica and silica-coated metal oxide) and biological (viruses) colloids were related to the surface properties of the colloids and aquifer grains (as measured by zeta potential). Excellent agreement was found between the extent of ferric oxyhydroxide surface coverage measured by electron microprobe and estimated by the collision efficiencies for the viruses. Increases in pH were most effective in mobilizing colloids (both natural and synthetic) and viruses because increases in pH above the pH_{pzc} were most effective in reversing the charge of the ferric oxyhydroxide coatings. In most cases, the transport of mobilized colloids was limited by the advance of the colloid-mobilizing agent (e.g., decrease in ionic strength, anionic surfactant concentration, reductant concentration). A notable exception occurred when pH was increased in one field experiment – mobilized colloids appear to have been transported ahead of the hydroxide plume owing to coating of colloids by natural organic matter. The field research led to the development of a new class of tracer colloids, silica-coated metal oxides. The size of the two types of colloids used in this research, silica-coated zirconia and titania, was controlled by varying the precipitation conditions.

The laboratory experiments examined the dependence of colloid transport and mobilization on chemical perturbations under controlled conditions and over a greater range of conditions. They showed that chemical perturbations that cause increasingly repulsive conditions produced more extensive and more rapid colloid release. A series of elevated pH experiments conducted on individual columns containing oriented, undisturbed sediments provided excellent data for the assessment of colloid release rates, a task that will be completed in the future. The laboratory experiments also showed that an increase of pH to too high a value produces less repulsion and, hence, less colloid release. This result duplicated a phenomenon observed in the field in the injection well of the highest pH injection.

The modeling effort aimed at simulating the processes controlling colloid transport in a contaminant plume focused on the development of a two-dimensional colloid transport model that considers the geochemical and physical heterogeneity of the porous medium as well as the dynamic aspects of particle deposition. While the modeling effort did not achieve the full objective of simulating the transport of colloids in a contaminant plume, major advances were made. Simulations of colloid transport in layered heterogeneous porous media indicate that both physical and geochemical heterogeneities play important roles in colloid

transport. Both types of heterogeneities can cause preferential flow of colloidal particles. The combination of layered physical heterogeneity and layered geochemical heterogeneity may enhance or reduce the preferential flow of colloids. Hence, physical and geochemical heterogeneities should be considered simultaneously in modeling colloidal transport in layered heterogeneous porous media. Overall, the numerical investigation based on the developed 2-D transport model provides a better understanding of colloid transport in physically and geochemically heterogeneous subsurface porous media. Experimental data of colloid transport in different heterogeneous porous media for laboratory or natural systems are needed to test the model predictions. Since the proposed model is more sophisticated than existing models for colloid transport in porous media, the application of this model will be affected by the availability of the model parameters. The identification of the model parameters in this 2-D model is important in applying this model in practice and will be addressed in future work.

Acknowledgments

We thank the following people for their help during this project: Bob Puls (U.S. EPA, R.S. Kerr Laboratory) for project guidance. Ron Harvey and Doug Kent (U.S. Geological Survey) for discussions on the project direction. Denis LeBlanc, Kathy Hess, and Tim McCobb (U.S. Geological Survey, Massachusetts District) for access to the field site and collection of sediment and groundwater samples. Mike Bonewitz (University of Colorado) and Jenny Baeseman (University of Wisconsin, Stevens Point) for field work. Jon Loveland (University of Colorado) for virus preparation. Dave Metge (U.S. Geological Survey) and Jon Larson and Dean Abadzic (University of Colorado) for data analysis. John Drexler (University of Colorado) for scanning electron microscopy. Phil Johnson (Notre Dame University) for streaming potential analysis.

QUALITY ASSURANCE STATEMENT

All research projects funded by the U.S. Environmental Protection Agency that make conclusions or recommendations based on environmentally related measurements are required to participate in the Agency Quality Assurance Program. This project was conducted under an approved Quality Assurance Program Plan and the procedures therein specified were used. Information on the plan and documentation of the quality assurance activities and results are available from the Principal Investigator.

DISCLAIMER

The U.S. Environmental Protection Agency through its office of Research and Development partially funded and collaborated in the research described here under Cooperative Agreement No. CR-824593 with the University of Colorado. It has been subjected to the Agency's peer and administrative review and it has been approved for publication as an EPA document. Mention of trade names or commercial products does not constitute endorsement or recommendation for use.

References

Abdel-Salam, A., and Chrysikopoulos, C. V., (1995) Modeling of colloid and colloid-facilitated contaminant transport in a two-dimensional fracture with spatially variable aperture. Transport in Porous Media, 20, 197-221.

Adamczyk, Z., Siwek, B., and Zembala, M., (1992) Reversible and irreversible adsorption of particles on homogeneous surfaces. Colloids Surf. A, 62, 119-130.

Allred, B. and Brown, G.O., (1994) Surfactant-induced reductions in soil hydraulic conductivity. Ground Water Monit. Remed. 174-184.

Amirbahman, A. and Olson, T.M., (1993) Transport of humic matter-coated hematite in packed beds. Environ. Sci. Technol., 27, 2807-2813.

Ard, R. A. (1997) Natural and artificial colloid mobilization in a sewage-contaminated aquifer: Field and laboratory experiments. M.S. Thesis, University of Colorado at Boulder, 202 pp.

Atherton, J.G. and Bell, S.S., (1983) Adsorption of viruses on magnetic particles--I. Adsorption of MS2 bacteriophage and the effect of cations, clay and polyelectrolyte. Water Res., 17, 943-948.

Backhus, D.A., Ryan, J.N., Groher, D.M., MacFarlane, J.K., and Gschwend, P.M., (1993) Sampling colloids and colloid-associated contaminants in ground water. Ground Water, 31, 466-479.

Bales, R.C., Hinkle, S.R., Kroeger, T.W., Stocking, K. and Gerba, C.P., (1991) Bacteriophage adsorption during transport through porous media: Chemical perturbations and reversibility. Environ. Sci. Technol., 25, 2088-2095.

Bales, R.C., Li, S., Maguire, K.M., Yahya, M.T., Gerba, C.P., and Harvey, R.W., (1995) Virus and bacteria transport in a sandy aquifer, Cape Cod, MA. Ground Water, 33, 653-661.

Barber L.B., II, Thurman, E.M., Schroeder, M.P. and LeBlanc, D.R., (1988) Long-term fate of organic micropollutants in sewage-contaminated groundwater. Environ. Sci. Technol., 22, 205-211.

Bellin, A., Salandin, P., and Rinaldo, R., (1992) Simulation of dispersion in heterogeneous porous formations: Statistics, first-order theories, convergence of computations. Water Resour. Res., 28(9), 2211-2227.

Bixby, R.L. and O'Brien, D.J., (1979) Influence of fulvic acid on bacteriophage adsorption and complexation in soil. Appl. Environ. Microbiol., 38, 840-845.

Black, T. C., and Freyberg, D. L., (1987) Stochastic modeling of vertically averaged concentration uncertainty in a perfectly stratified aquifer. Water Resour. Res., 23, 997-1004.

Bosma, W. J., and van der Zee, S. E. A. T. M., (1993) Transport of reacting solute in a one-dimensional, chemically heterogeneous porous medium. Water Resour. Res., 29(1), 117-131.

Buddemeier, R.W. and Hunt, J.R., (1988) Transport of colloidal contaminants in groundwater: Radionuclide migration at the Nevada Test Site. Appl. Geochem. 3, 535-548.

Burge, W.D. and Enkiri, N.K., (1978) Virus adsorption by five soils. J. Environ. Qual., 7, 73-76.

Charney, J., Machlowitz, R.A., and Spicer, D.S., (1962) The adsorption of poliovirus antigen to glass surfaces. Virology, 18, 495-497.

Chrysikopoulos, C. V., Kitanidis, P. K., and Roberts, P. V., (1990) Analysis of one-dimensional solute transport through porous media with spatially variable retardation factor. Water Resour. Res., 26, 437-446.

Corapcioglu, M. Y., and S. H. Kim (1995) Modeling facilitated contaminant transport by mobile bacteria. Water Resour. Res., 31(11), 2639-2647.

Coston, J.A., Fuller, C.C., and Davis, J.A., (1995) Pb2+ and Zn2+ adsorption by a natural aluminum- and iron-bearing surface coating on an aquifer sand. Geochim. Cosmochim. Acta, 59, 3535-3547.

Dagan, G. (1984) Solute transport in heterogeneous porous formations. J. Fluid Mech., 145, 151-177.

Davis, J.A. (1982) Adsorption of natural dissolved organic matter at the oxide/water interface. Geochim. Cosmochim. Acta, 46, 2381-2393.

Degueldre, C., Baeyens, B., Goerlich, W., Riga, J., Verbist, J., and Stadelmann, P., (1989) Colloids in water from a subsurface fracture in granitic rock, Grimsel Test Site, Switzerland. Geochim. Cosmochim. Acta, 53, 603-610.

Dick, S.G., Fuerstenau, D.W., and Healy, T.W., (1971) Adsorption of alkylbenzene sulfonate (A.B.S.) surfactants at the alumina-water interface. J. Colloid Interface Sci., 37, 595-602.

Dunnivant, F., Schwarzenbach, R.P., and Macalady, D., (1992) Reduction of substituted nitrobenzenes in aqueous solutions containing natural organic matter. Environ. Sci. Technol., 26, 2133-2141.

Elimelech, M., Gregory, J., Jia, X., and Williams, R., (1995) Particle Deposition & Aggregation, Butterworth-Heinemann Ltd.

Elimelech, M., and Song, L., (1992) Deposition of colloids in porous media: Theory and numerical solution. In Transport and Remediation of Subsurface Contaminants: Colloidal, Interfacial, and Surfactant Phenomena, D. A. Sabatini and R. C. Knox, Eds.; American Chemical Society Symposium Series, 491, 26-39.

Elimelech, M. (1991) Kinetics of capture of colloidal particles in packed beds under attractive double layer interactions. J. Colloid Interface Sci., 146, 337-352.

Elimelech, M., and O'Melia, C. R., (1990) Kinetics of deposition of colloidal particles in porous media. Environ. Sci. Technol., 24, 1528-1536.

Farrah, S.R. and Preston, D.R., (1991) Adsorption of viruses by diatomaceous earth coated with metallic oxides and metallic peroxides. Water Sci. Technol., 24, 235-240.

Freeze, R. A. (1975) A stochastic-conceptual analysis of one-dimensional groundwater flow in nonuniform homogeneous media. Water Resour. Res., 11(5), 725-741.

Fuhs, G.W., Chen, M., Sturman, L.S., and Moore, R.S., (1985) Virus adsorption to mineral surfaces is reduced by microbial overgrowth and organic coatings. Microb. Ecol., 11, 25-39.

Garabedian, S. P., Leblanc, D. R., Gelhar, L. W., and Celia, M. A., (1991) Large-scale natural gradient tracer test in sand and gravel, Cape Cod, Massachusetts, 2, Analysis of spatial moments for a nonreactive tracer. Water Resour. Res., 27, 911-924.

Gelhar, L. W., Welty, C., and Rehfeldt, K. R., (1992) A critical review of data on field-scale dispersion in aquifers. Water Resour. Res., 28(7), 1955-1974.

Gelhar, L. W., and Axness, C. L., (1983) Three-dimensional stochastic analysis of macrodispersion in aquifers. Water Resour. Res., 19(1), 161—180.

Gelhar, L. W., A. L. Gutiahr, and R. L. Naff (1979) Stochastic analysis of macrodispersion in stratified aquifer. Water Resour. Res., 15(6), 1387-1397.

Gerba, C.P. (1984) Applied and theoretical aspects of virus adsorption to surfaces. Adv. Appl. Microbiol., 30, 133-169.

Gerba, C.P., Goyal, S.M., Cech, I., and Bogdan, G.F., (1981) Quantitative assessment of the adsorptive behavior of viruses to soils. Environ. Sci. Technol., 15, 940-944.

Goldenberg, L.C., Magaritz, M., and Mandel, S., (1983) Experimental investigation on irreversible changes of hydraulic conductivity on the seawater-freshwater interface in coastal aquifers. Water Resour. Res., 19, 77-85.

Grolimund, D., Borkovec, M., Barmettler, K., and Sticher, H., (1996) Colloid-facilitated transport of strongly sorbing contaminants in natural porous media: A laboratory column study. Environ. Sci. Technol., 30(10), 3118-3123.

Harmand, B., Rodier, E., Sardin, M., and Dodds, J., (1996) Transport and capture of submicron particles in s natural sand: short column experiments and a linear model. Colloids and Surfaces A 107, 233-244.

Harvey, R.W. and Garabedian, S.P. ,(1991) Use of colloid filtration theory in modeling movement of bacteria through a contaminated sandy aquifer. Environ. Sci. Technol., 25, 178-185.

Harvey, R.W., George, L.H., Smith, R.L., and LeBlanc, D.R. (1989) Transport of microspheres and indigenous bacteria through a sandy aquifer: Results of natural- and forced-gradient tracer experiments. Environ. Sci. Technol., 23, 51-56.

Harvey, R.W., Kinner, N.E., Bunn, A., MacDonald, D., and Metge, D., (1995) Transport behavior of groundwater protozoa and protozoan-sized microspheres in sandy aquifer sediments. Appl. Environ. Microbiol., 61, 209-217.

Heron, G., Crouzet, C.A., Bourg, C. M., and Christensen, T. H., (1994) Separation of Fe(II) and Fe(III) in contaminated aquifer sediments using chemical extraction techniques. Environ. Sci. Technol., 28, 1698-1705.

Hess, K.H., Wolf, S.H. and Celia, M.A., (1992) Large-scale natural gradient tracer test in a sand and gravel aquifer, Cape Cod, Massachusetts 3. Hydraulic conductivity variability and calculated macrodispersivities. Water Resour. Res., 28, 2011-2027.

Hess, K. M. (1989) Use of borehole flowmeter to determine spatial heterogeneity of hydraulic conductivity and macrodispersivity in a sand and gravel aquifer, Cape Cod, Massachusetts, paper presented at NWWA Conference on New Field Techniques for Qualifying the Physical and Chemical properties of Heterogeneous Aquifers Natl. Water Well Assoc., Houston, Tex.

Higgo, J. J. W., Williams, G. M., Harrison, I., Warwick, P., Gardiner, M. P., and Longworth G. , (1993) Colloid transport in a glacial sand aquifer- laboratory and field studies. Colloids Surf. A 73, 179-200.

Hoeskema, R. J., and Kitanidis, P. K., (1984) An application of the geostatistical approach to the inverse problem in two-dimensional groundwater modeling. Water Resour. Res., 20(7), 1003-1020.

Hufschmied, P. (1986) Estimation of three-dimensional statistically anisotropic hydraulic conductivity field by means of single well pumping tests combined with flowmeter measurements. Hydrogeologie, 2, 163-174.

Johnson, P.R., Sun, N. and Elimelech, M., (1996) Colloid transport in geochemically heterogeneous porous media: Modeling and measurements. Environ. Sci. Technol., 30, 3284-3293.

Johnson, P. R., and M. Elimelech (1995) Dynamics of colloid deposition in porous media: Blocking based on random sequential adsorption. Langmuir, 11, 801-812.

Kent, D.B., Davis J.A., Anderson L.C.D., Rea B.A. and Waite T.D. (1994) Transport of chromium and selenium in the suboxic zone of a shallow aquifer: Influence of redox and adsorption reactions. Water Resour. Res., 30, 1099-1114.

Khilar, K.C. and Fogler, H.S., (1984) The existence of a critical salt concentration for particle release. J. Colloid Interface Sci., 101, 214-224.

Kolakowski, J.E. and Matijevic, E., (1979) Particle adhesion and removal in model systems Part 1.--Monodispersed chromium hydroxide on glass. J. Chem. Soc. Faraday Trans. I 75, 65-78.

Kretzschmar, R., Robarge, W.P. and Amoozegar, A., (1995) Influence of natural organic matter on colloid transport through saprolite. Water Resour. Res., 31, 435-445.

Lapidus, L., and Amundson, N.R., (1952) Mathematics of adsorption in beds. VI, The effect of longitudinal diffusion in ion exchange and chromatographic columns. J. Phys. Chem., 56, 984-988.

LeBlanc, D. R. (1984) Sewage plume in a sand and gravel aquifer, Cape Cod, Massachusetts. U.S. Geol. Survey Water Supply Paper 2218, 28 pp.

LeBlanc, D.R., Garabedian, S.P., Hess, K.H., Gelhar, L.W., Quadri, R.D., Stollenwerk, K.G. and Wood, W.W., (1991) Large-scale natural gradient tracer test in sand and gravel, Cape Cod, Massachusetts 1. Experimental design and observed tracer movement. Water Resour. Res., 27, 895-910.

Leij, F. J., and Dane, J. H. , (1990) Analytical solutions of the one-dimensional advection equation and two- or three-dimensional dispersion equation. Water Resour. Res., 26(7), 1475-1482.

Liang, L. and Morgan, J.J. ,(1990) Chemical aspects of iron oxide coagulation in water: Laboratory studies and implications for natural systems. Aquatic Sciences 52, 32-55.

Lindqvist, R., and Enfield, C. G., (1992) Cell density and non-equilibrium sorption effects on bacteria dispersal in groundwater microcosms. Microb. Ecol., 24, 25-41.

Liu, H. H., and Molz, F. J., (1997) Comment on “Evidence for non-Gaussian scaling behavior in heterogeneous sedimentary formations” by Scott Painter. Water Resour. Res., 33(4), 907-908.

Loveland, J.P., Ryan, J.N., Amy, G.L. and Harvey, R.W. (1996) The reversibility of virus attachment to mineral surfaces. Colloids Surf. A 107, 205-221.

Magelky, R. D. (1998) Colloid deposition and mobilization in a sewage-contaminated iron oxide-coated aquifer. M.S. Thesis, University of Colorado, Boulder, 235 pp.

Mantoglou, A., and Wilson, J. L., (1982) The turning bands method for simulation of random fields using line generation by a spectral method. Water Resour. Res., 18(5), 1379-1394.

McCarthy, J. F., and Degueldre, C., (1993) Sampling and characterization of colloids and particles in groundwater for studying their role in contaminant transport. In Environmental Particles, Environmental Analytical and Physical Chemistry Series, Buffle, J., and H. P. van Leeuwen (Eds.), Lewis Publishers.

McCarthy, J. F., and Zachara, J. M., (1989) Subsurface transport of contaminants. Environ. Sci. Technol., 23, 496-502.

McDowell-Boyer, L.M. (1992) Chemical mobilization of micron-sized particles in saturated porous media under steady flow conditions. Environ. Sci. Technol., 26, 586-593.

Mills A.L., Herman, J.S., Hornberger, G.M. and DeJesús, T.H. (1994) Effect of solution ionic strength and iron coatings on minerals grains on the sorption of bacterial cells to quartz sand. Appl. Environ. Microbiol., 60, 3300-3306.

Moltyaner, G. L. (1986) Stochastic versus deterministic: A case study. Hydrogeologie, 2, 183-196.

Molz, F. L., Güven, O., Melville, J. G., Crocker, R. D., and Matteson, K. T., (1986) Performance, analysis, and simulation of a two-well tracer test at the Mobile site. Water Resour. Res., 22(7), 1031-1037.

Moore, R.S., Taylor, D.H., Reddy, M.M.M. and Sturman, L.S. (1982) Adsorption of reovirus by minerals and soils. Appl. Environ. Microbiol., 44, 852-859.

Moore, R.S., Taylor, D.H., Sturman, L.S., Reddy, M.M. and Fuhs, G.W. (1981) Poliovirus adsorption by 34 minerals and soils. Appl. Environ. Microbiol., 42, 963-975.

Mukerjee, P. and Mysels, K. J., (1971) Critical micelle concentrations of aqueous surfactant systems. NSRDS-NBS 36. Washington, DC, National Bureau of Standards, 227 pp.

Murray, J.P. and Parks, G.A., (1980) Poliovirus adsorption on oxide surfaces. Correspondence with the DLVO-Lifshitz theory of colloid stability. In Particulates in Water. Characterization, Fate, Effects, and Removal (Kavanaugh M.C. and Leckie J.O., Eds.), p. 97. American Chemical Society, Washington, DC.

Nightingale, H.I. and Bianchi , W.C., (1977) Ground-water turbidity resulting from artificial recharge. Ground Water, 15, 146-152.

Olsen, R.H., Siak, J.-S. and Gray, R.H. (1974) Characteristics of PRD1, a plasmid-dependent broad host range DNA bacteriophage. J. Virology, 14, 689-699.

Painter, S. (1996) Evidence for non-Gaussian scaling behavior in heterogeneous sedimentary formations. Water Resour. Res., 32(5), 1183-1195.

Painter, S. (1997) Reply. Water Resour. Res., 33(4), 909-909.

Parks, G.A. (1965) The isoelectric points of solid oxides, solid hydroxides, and aqueous hydroxo complex systems. Chem. Rev., 65, 177-198.

Parks, G.A. (1967) Aqueous surface chemistry of oxides and complex oxide minerals. In Equilibrium Concepts in Natural Water Systems (Stumm W., Ed.), p. 121. American Chemical Society, Washington, DC.

Penrod, S.L., Olson, T.M., and Grant, S.B., (1996) Deposition kinetics of two viruses in packed beds of quartz granular media. Langmuir 12, 5576-5587.

Pieper, A.P., Ryan, J.N., Harvey, R.W., Amy, G.L., Illangasekare, T.H., and Metge, D.W., (1997) Transport and recovery of bacteriophage PRD1 in a sand and gravel aquifer: Effect of sewage-derived organic matter. Environ. Sci. Technol., 31, 1163-1170.

Privman, V., Frisch, H. L., Ryde, N., and Matijevic, E., (1991) Particle adhesion in model system. 13. Theory of multilayer deposition. J. Chem. Soc. Faraday Trans., 87(9), 1371-1375.

Puls, R.W., Clark, D.A., Bledsoe, B., Powell, R.M. and Paul, C.J., (1992) Metals in ground water: sampling artifacts and reproducibility. Haz. Waste Haz. Mat., 9, 149-162.

Puls, R.W. and Powell, R.M., (1992) Transport of inorganic colloids through natural aquifer material: Implications for contaminant transport. Environ. Sci. Technol., 26, 614-621.

Rajagopalan, R. and Tien, C., (1976) Trajectory analysis of deep-bed filtration with the sphere-in-cell porous media model. AIChE J. 22, 523-533.

Redman, J.A., Grant, S.B., Olson, T.M., Hardy, M.E. and Estes, M.K., (1997) Filtration of recombinant Norwalk virus particles and bacteriophage MS2 in quartz sand: Importance of electrostatic interactions. Environ. Sci. Technol., 31, 3378-3383.

Roy, S.B. and Dzombak, D.A. ,(1996) Colloid release and transport processes in natural and model porous media. Colloids Surf. A 107, 245-262.

Ryan, J.N., Ard, R.A., Magelky, R.D., and Elimelech, M., (in preparation) Effect of elevated pH on the mobilization of colloids from a ferric oxide-coated quartz sand: Laboratory and field experiments. To be submitted to Environmental Science and Technology.

Ryan, J.N. and Elimelech, M., (1996) Colloid mobilization and transport in groundwater. Colloids Surf. A 107, 1-52.

Ryan, J.N., Elimelech, M., Ard, R.A., Harvey, R.W., and Johnson, P.R., (1999) Bacteriophage PRD1 and silica colloid transport and recovery in an iron oxide-coated sand aquifer. Environ. Sci. Technol., 33, 63-73.

Ryan, J.N. and Gschwend, P.M., (1990) Colloid mobilization in two Atlantic Coastal Plain aquifers: Field studies. Water Resour. Res., 26, 307-322.

Ryan, J.N. and Gschwend, P.M., (1991) Extraction of iron oxides from sediments using reductive dissolution by titanium(III). Clays Clay Min., 39, 509-518.

Ryan, J.N. and Gschwend, P.M., (1994) Effects of solution chemistry on clay colloid mobilization from an iron oxide-coated sand aquifer. Environ. Sci. Technol., 28, 1717-1726.

Ryan, J.N., Magelky, R.D., and Elimelech, M., (in preparation) Using silica-coated metal oxide tracer colloids of variable size in a colloid transport field experiment. To be submitted to Colloids and Surfaces A. Physicochemical and Engineering Aspects.

Saiers, J. E., Hornberger, G. M., and Harvey, C., (1994) Colloidal silica transport through structured, heterogeneous porous media. J. Hydrology, 163, 271-288.

Scholl, M.A. and Harvey, R.W. (1992) Laboratory investigations on the role of sediment surface and groundwater chemistry in transport of bacteria through a contaminated sandy aquifer. Environ. Sci. Technol. 26, 1410-1417.

Small, D.A. and Moore, N.F. (1987) Measurement of surface charge of baculovirus polyhedra. Appl. Environ. Microbiol., 53, 598-602.

Smith, R.L., Howes, B.L. and Garabedian, S.P. (1991) In-situ measurement of methane oxidation in groundwater using a natural gradient tracer test. Appl. Environ. Microbiol., 57, 1997-2004.

Sobsey, M.D., Dean, C.H., Knuckles, M.E., and Wagner, R.A., (1980) Interactions and survival of enteric viruses in soil materials. Appl. Environ. Microbiol., 40, 92-101.

Song, L., and M. Elimelech (1994) Transient deposition of colloidal particles in heterogeneous porous media. J. Colloid and Interface Sci., 167, 301-313.

Song, L., Johnson, P.R., and Elimelech, M., (1994) Kinetics of colloid deposition onto heterogeneously charged surfaces in porous media. Environ. Sci. Technol., 28, 1164-1171.

Sudicky, E. A. (1986) A natural gradient experiment on solute transport in a sand aquifer: Spatial variability of hydraulic conductivity and its role in the dispersion process. Water Resour. Res., 22(13), 2069-2082.

Sun, N. (1998) Colloid transport in physically and geochemically heterogeneous subsurface porous media, Ph.D. Thesis, University of California at Los Angeles.

Sun, N., Elimelech, M., Sun, N.-Z., and Ryan J.N. (submitted) Colloid transport in physically and geochemically heterogeneous subsurface porous media: 1. A two dimensional model. Submitted to Water Resources Research.

Stumm, W., and Morgan, J. J., (1995) Aquatic Chemistry, 3rd Ed. Wiley-Interscience: New York.

Sun, Ne-Zheng (1995) Mathematical Modeling of Groundwater Pollution, Springer-Verlag, New York.

Sun, Ne-Zheng, and Yeh, W. W.-G., (1983) A proposed upstream weight numerical method for simulating pollutant transport in groundwater. Water Resour. Res., 19(6), 1489-1500, 1983.

Tobiason, J. E. (1989) Chemical effects on the deposition of non-Brownian particles. Colloids Surf., 39, 53-77, 1989.

Tompson, A. F. B., Ababou, R., and Gelhar, L. W., (1989) Implementation of the three dimensional turning bands random field generator. Water Resour. Res., 25(10), 2227-2243, 1989.

Walter, D. A., Rea, B. A., Stollenwerk, K. G., and Savoie, J. (1996) Geochemical and hydrologic controls on phosphorus transport in a sewage-contaminated sand and gravel aquifer near Ashumet Pond, Cape Cod, Massachusetts. U.S. Geol. Survey Water-Supply Paper 2463, 89 pp.

Yao K.-M., Habibian, M.T. and O'Melia, C.R. (1971) Water and wastewater treatment filtration: Concepts and applications. Environ. Sci. Technol. 5, 1105-1112.